GDAŃSK UNIVERSITY OF TECHNOLOGY

INSTITUTE OF NAVAL ARCHITECTURE AND OCEAN ENGINEERING

Polish Maritime Research

No 4 (112) 2021
Vol. 28

ADDRESS OF PUBLISHER & EDITOR'S OFFICE:

GDAŃSK UNIVERSITY OF TECHNOLOGY

Institute of Naval Architecture and Ocean Engineering
G. Narutowicza 11/12
80-233 Gdańsk, POLAND

Price:
single issue: 25 PLN

Prices for abroad
single issue:
- in Europe EURO 15
- overseas USD 20

WEB:
pg.edu.pl/pmr

e-mail : pmr@pg.edu.pl

ISSN 1233-2585

CONTENS

ADDRESS OF PUBLISHER & EDITOR'S OFFICE:

GDAŃSK UNIVERSITY OF TECHNOLOGY

Institute of Naval Architecture and Ocean Engineering
G. Narutowicza 11/12
80-233 Gdańsk, POLAND

Editorial

POLISH MARITIME RESEARCH is the scientific journal with a worldwide circulation. This journal is published quarterly (four times a year) by Gdansk University of Technology (GUT). On September, 1994, the first issue of POLISH MARITIME RESEARCH was published. The main objective of this journal is to present original research, innovative scientific ideas, and significant findings and application in the field of **:**

Naval Architecture, Ocean Engineering and Underwater Technology,

The scope of the journal covers selected issues related to all phases of product lifecycle and corresponding technologies for offshore floating and fixed structures and their components.

All researchers are invited to submit their original papers for peer review and publications related to methods of the design; production and manufacturing; maintenance and operational processes of such technical items as:

- all types of vessels and their equipment,
- fixed and floating offshore units and their components,
- autonomous underwater vehicle (AUV) and remotely operated vehicle (ROV).

We welcome submissions from these fields in the following technical topics:

- ship hydrodynamics: buoyancy and stability; ship resistance and propulsion, etc.,
- structural integrity of ship and offshore unit structures: materials; welding; fatigue and fracture, etc.,
- marine equipment: ship and offshore unit power plants: overboarding equipment; etc.

sciendo

POLISH MARITIME RESEARCH 4 (112) 2021 Vol. 28; pp. 63-87
10.2478/pomr-2021-0050

PERFORMANCE AND EMISSION MODELLING AND SIMULATION OF MARINE DIESEL ENGINES USING PUBLICLY AVAILABLE ENGINE DATA

Mohammad Hossein Ghaemi*
Gdańsk University of Technology, Poland
* Corresponding author: *ghaemi@pg.edu.pl (M.H. Ghaemi)*

ABSTRACT

To analyse the behaviour of marine diesel engines in unsteady states for different purposes, for example to determine the fuel consumption or emissions level, to adjust the control strategy, to manage the maintenance, etc., a goal-based mathematical model that can be easily implemented for simulation is necessary. Such a model usually requires a wide range of operating data, measured on a test stand. This is a time-consuming process with high costs and the relevant data are not available publicly for a selected engine. The present paper delivers a rapid and relatively simple method for preparing a simulation model of a given marine diesel engine, based only on the widely available data in the project guides indicated for steady state conditions. After establishing the framework of the mathematical model, it describes how the parameters of the model can be adjusted for the simulation model and how the results can be verified as well. Conceptually, this is a trial and error method, but the presented case example makes clear how the parameters can be selected to reduce the number of trials and quickly determine the model parameters. The necessary descriptions are given through a case study, which is the MAN-B&W 8S65ME-C8 marine diesel engine. The engine is assumed to be connected to a constant pitch propeller. The presented mathematical model is a mean-value zero-dimensional type with seven state variables. The other variables of the engine are determined based on the state independent variables and the input value, which is the fuel rate. The paper can be used as a guideline to prepare a convenient mathematical model for simulation, with the minimum publicly available data.

Keywords: Marine diesel engine,Mathematical model,Mean-Value Model,Simulation of ship propulsion system

INTRODUCTION

DEFINITION OF THE PROBLEM

The modelling and simulation of marine diesel engines, their performance and unsteady state behaviour have been extensively taken into consideration during the last several decades. In recent years, more attention has been paid to determining the emissions induced by these engines, regarding their role in the production of air pollutants, mainly SO_x, CO_x, NO_x, soot and particulate matter (PM). NOx and soot depend directly on the operational condition of a diesel engine, and the rest firstly depend on the applied fuel and its components and then on the engine operational features. The parameters of the available mathematical models for simulation of diesel engines are mainly selected or adjusted using the data delivered by the engine manufacturers, which are usually measured on a test stand. In the detailed models the number, types and volume of the required data for adjusting the model parameters are high, and without enough measured data in the stand tests it is usually impossible to prepare a reliable simulation model for the given engine. On the other hand, the project guides delivered by the engine manufacturers usually do not include the data necessary for simulation of the performance of the diesel engine in transient conditions. This is a fundamental

problem for researchers, who are interested in simulating the behaviour of diesel engines in unsteady conditions. The results of such an investigation, in turn, are often required for better understanding of the interactions, for example, in the case of propeller-engine, hull-propeller-engine or hull-rudder-propeller-engine interactions, fuel consumption, combustion efficiency, emissions induced by the engine operation, control purposes, etc., see for example [1, 2, 3, 4, 5, 6].

LITERATURE REVIEW

There are many methods for the modelling of a ship propulsion system and particularly the transient behaviour of marine diesel engines, delivered in different studies. They vary from advanced models that calculate the details of internal processes such as the turbulence in receivers (manifolds) and cylinders, the effect of lubrication oil flow, changes in the chemical properties of exhaust gas components etc., to a simple single first-order system.

While the choice of the model to be used is usually based on the main goal of the modelling, nowadays, because of the availability of cheaper and accessible computational power, the major restriction on the complexity of the model to be simulated depends only on the availability of suitable data. In fact, the most time-consuming part is setting up the parameters of a simulation model, which usually consists of data collection, data analysis and filtering, and then the determination of various parameters of the model.

Excluding Artificial Intelligence (AI) and Neural Networks (ANN) identification methods, generally five groups of modelling methods can be found in the literature, while the majority of the delivered models are combinations of two or more methods. These methods and their historical background are described below and after that a short literature review on marine diesel engine modelling focusing on recent publications is delivered.

1. First-order and sometimes time-delayed model, e.g.:

$$G(s) = \frac{K \cdot e^{-T_0 s}}{1 + \tau s} = \frac{Q(s)}{H(s)} \tag{1}$$

where K is gain, T_0 is time delay, τ is a time constant, and Q and H represent the engine torque and fuel rate (or rack), respectively. In this case, the diesel engine has been considered as a black box and the internal events cannot be expressed using such a model. It is a linear model suitable, for example, in the case of ship positioning or manoeuvring models. The linearity of the model limits its application to a narrow range of operation. Gajek presented such a simple model of a diesel engine for use in the ship's dynamic model [7]. Andersen [8], Roszczyk et al. [9], Tittenbrun [10], Kowalski et al. [11] and Krutov [12] delivered some similar models, which they applied for engine transient response, ship electrical net analysis and control system studies.

2. Models based on identification methods. These are usually built according to statistical estimations. Although making a non-linear model using statistical methods is theoretically possible, the author could not find any study applying such a model directly. Additionally, only a few linear statistical-based models have been reported. It is a unique method and a very large number of experimental data are required, therefore it is time-consuming and costly. Generally, a set of transfer functions are selected and their gains, parameters and coefficients are fitted to experimental test results. The model presented by Blanke and Andersen is an example of such a model [13]. Lam delivered a model that is performed using statistical-based methods for analysis of the diesel engine transient response [14].
3. Mean-value quasi-steady models make up the third group. The major limitation of the simple methods described above is the heavy reliance on a large fund of accurate engine data, and usually over a wide range of operation. When the goal is realistic modelling of unsteady phenomena, it can be achieved by assuming quasi-steady characteristics, where, at each instant, the characteristics are the same as in the related steady state. The engine set is divided into components, the engine as prime mover, inlet air and exhaust gas receivers, compressor and turbine, charge air cooler, etc. As a result, the approach of dividing the engine set into physical blocks is realised by representing each functional block by one or more equations or by employing look-up tables. However, the engine cylinders are still modelled as a black box and the inputs to the engine are fuel and air, while the output is exhaust gas. Therefore, only mean values of the engine variables can be calculated. The mean-value models reported by Ferenc et al. are adequate examples of such a method for medium-speed diesel engine application [15, 16, 17]. Smith [18], Taylor [19] and Ford [20] delivered some simplified and linearised mean-value models. Woodward and Lattore [21, 22], Hendricks et al. [23, 24, 25, 26], Jansen [27], Woud 28], Próchnicki [29, 30], also Próchnicki and Dzida [31] and lastly Kafar [32] presented transient simulation models of diesel engines and their application according to the mean-value method. Lan et al. presented a mean value quasi-steady model for analysis of the control system of a ship propulsion plant, but they concentrated on high- and medium-speed diesel engines [33].
4. Zero-dimensional instantaneous quasi-steady models are the fourth group of models. The difference between this model and the previous group is that here the internal events of engine cylinders are modelled in addition. These internal variables are mainly related to the mass and temperature of the working fluid during different engine operational processes. The most relevant examples of such an internal process are ignition and combustion. However, the variation of the gas state (for example, pressure and temperature), especially along the exhaust gas receiver (manifold) when a pulse turbocharger system is applied, has been ignored. In other words, the working fluid state at each treated component is instantaneously constant and the flow is homogeneous. In this regard, such a model is called

"zero-dimensional" or sometimes a "cycle model". Olsen in 1958 reported on the development of a simulation model of a free piston engine [34]. Cook one year later published results generated by a cycle simulation model for a turbocharged diesel engine [35]. Whitehouse et al. in 1962 reported on a diesel engine cycle model, which considered in detail the full four-stroke cycle [36]. The single-cylinder model developed by Borman advanced the state-of-the-art considerably at the time of reporting in 1964 [37]. Six years later, Streit [38] extended the zero-dimensional model of Borman to accommodate a large two-stroke turbocharged diesel. In 1976 Marzouk improved the latter delivered version [40]. Later on Benson [41], Woschni [42, 43], Wiebe [44], and Watson [45, 46] published the results of a major development extending the 0-D concept to embrace transient simulation especially due to combustion and heat transfer aspects. Next, Banisoleiman et al. [47], Larmi [48] and Ghaemi [49] presented two advanced 0-D instantaneous quasi-steady models for modern long-stroke low- and medium-speed diesel engine transient response.

5. The last group of models is one-dimensional instantaneous quasi-steady. The available models of this group are very similar to the zero-dimensional quasi-steady models with one difference, which is variation of the working fluid state also in each individual component. In other words, the gas state can be illustrated not only as a function of time but also as a function of geometrical position, continuously, i.e., the system parameters and variables are not lumped but distributed. Benson in spent much time at the end of the 1950s using the graphical Method of Characteristics (MOC) to solve the 1-D unsteady flow equations for a two-stroke marine diesel exhaust system [50]. Later on Benson et al. [51, 52] developed this model. Blair et al. presented a complete engine model based on the MOC solution of the 1-D unsteady flow equations but concentrated on high-speed, high specific output two- and four-stroke applications [53, 54, 55, 56, 57]. Bazari in 1992 published a 1-D unsteady flow model for simulation of NOX and SOX emissions of a low-speed diesel engine [56]. In recent years, the attention of researchers has been mainly focused on the modelling of marine diesel engines for fuel consumption and emission reduction, better control of the performance of the engine or its components, increasing the energy efficiency of the ships, better description of the internal phenomena, particularly ignition and combustion processes, adequate matching of the engine and turbocharger, enhancing the simulation models for newly delivered solutions such as engines with alternative fuels, for instance LNG, biofuels, methanol or similar, dual-fuel systems, application of hybrid propulsion systems, etc. These new needs and questions have generated a wide series of studies and publication of their results. A systematic review on the modelling of diesel engines for simulation and control can be found in [57].

Taking into account the possibilities that a mean-value model can bring to the research, which needs a model of the engine as part of a wider range model, recently more attention has been paid to this type of model; see, for example, Lee [58], Hendricks [59], Sengupta [60], Yacoub [61], Theotokatos [62], Guzzella [63], Yum [64], Scappin [65], Kharroubi [66], Baldi [67], Altosole et al. [68].

THE GOAL AND STRUCTURE

The main goal and new dimension of this paper is delivering a simple and practical method that can be rapidly applied for adjusting the parameters of a mean-value zero-dimensional model of a marine diesel engine without any need for access to the detailed, time-consuming and costly data that are taken from stand test results or have probably been recorded for a real installed engine on board a ship. This should enable researchers and engineers to identify the necessary parameters of the mathematical model and also verify the results based on the publicly available data in the project guides.

The structure of the paper is as follows: first, a general framework of a zero-order mean-values analytical model of a marine diesel engine is established and presented. Next, it is shown in a stepwise manner how to adjust the model parameters for a wide engine operational range, from 10% to 100% of MCR. Then, the parameter adjustment method is applied for a selected marine diesel engine, MAN-B&W 8S65ME-C8. Finally, the results of simulation are verified based on the available steady-state characteristics to check the accuracy of the adjusted parameters.

THE MEAN-VALUE MATHEMATICAL MODEL OF MARINE DIESEL ENGINE

The main components of a marine diesel engine are the turbocharger, charge air cooler, inlet air manifold or receiver, cylinders, fuel supply mechanism and exhaust gas receiver. This is shown in Fig. 1. Air is taken by the compressor of the turbocharger at point 0 at atmospheric pressure and temperature (p_{at} and T_{at}) and is compressed and delivered to a charge air cooler by passing point 1 to reduce the temperature, increase the density and enable the cylinders to be supplied with a larger amount of air. After passing point 2, the accumulated air in the inlet air manifold (or receiver), which can be integrated into the charge air cooler, has the mass and temperature indicated by m_{am} and T_{am}, respectively. The cylinders are charged by the compressed air and the fuel, where the latter can be identified by the mass fuel rate, $\dot{m}_f$, induced by the fuel rack, X_f. As a result, the engine torque M_e is delivered to the connecting shaft at the angular velocity of ω. After combustion, the exhaust gases pass point 4 and accumulate at the exhaust gas receiver. The mass and temperature of the exhaust gases in this receiver

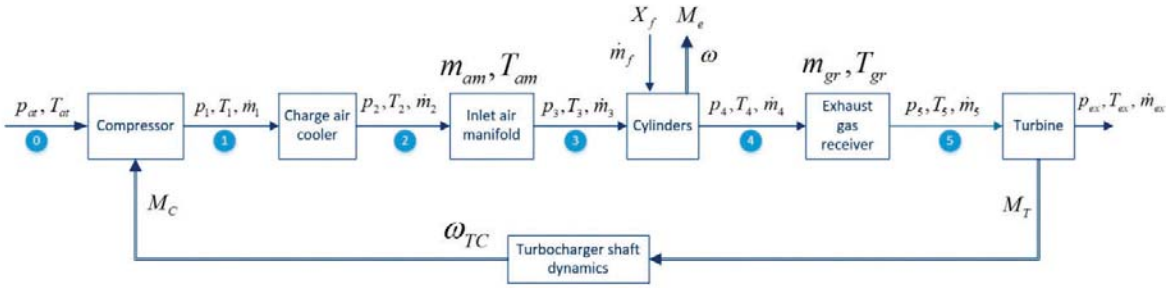

Fig. 1. Schematic illustration of a marine diesel engine's components and its variables at different points

are m_{gr} and T_{gr}, respectively. Next, the exhaust gases rotate the turbine of the turbocharger to generate the required power by the compressor. The turbine torque, M_T, and compressor torque, M_C, are equal at steady states, but during unsteady states the difference between them causes changes in the angular velocity of the turbocharger shaft, ω_{TC}, based on Newton's second law of angular motion. The pressures, temperatures and mass flow rate of air or exhaust gases at each point are indicated by p, T, and $\dot{m}$ with a lower index that reflects the number of the considered point.

The following assumptions have been applied:

1. The losses in the flow rates due to leakages are negligible.
2. The pressure, temperature and specific volume at point 3 have the same respected values as in the intake air manifold.
3. The inlet air pressure and its mass flow rate are not changed between points 2 and 3, and the air cooler changes only the temperature of the air.
4. The pressures at points 4 and 5 are equal and are the same as the pressure of the exhaust gas receiver.
5. The temperature and specific volume of the exhaust gases through the turbine are not changed and are the same as the respected values for the exhaust gas receiver.
6. Both the air and exhaust gases are assumed to be semi-ideal gases.

These assumptions reduce the number of state variables, when the required accuracy of the simulation results can be satisfied with no significant deviation in comparison to the real case.

TURBINE

Mass flow rate of exhaust gases into the turbine

The mass flow rate of exhaust gases intro the turbine can be modelled as an isentropic ideal gas flow through a converging-diverging nozzle with an equivalent cross-section area of A_T^*:

$$\dot{m}_5 = A_T^* \cdot \psi_T \cdot \sqrt{P_{gr} \cdot \rho_{gr}} \tag{2}$$

Hence ψ_T is the turbine flow function, which depends on the adiabatic exponent (heat capacity ratio), κ_T:

$$\psi_T(\pi_T) = \begin{cases} \left[\dfrac{2\kappa_T}{\kappa_T - 1} \left(\pi_T^{\frac{2}{\kappa_T}} - \pi_T^{\frac{\kappa_T+1}{\kappa_T}} \right) \right]^{\frac{1}{2}} & ; \quad \pi_T \geq \pi_{T\,cr.} \\ \left[\kappa_T \cdot \left(\dfrac{2}{\kappa_T + 1} \right)^{\frac{\kappa_T+1}{\kappa_T-1}} \right]^{\frac{1}{2}} & ; \quad \pi_T < \pi_{T\,cr.} \end{cases} \tag{3}$$

where

$$\pi_{T\,cr.} = \left(\frac{2}{\kappa_T + 1} \right)^{\frac{\kappa_T}{\kappa_T - 1}} \tag{4}$$

A_T^* is the equivalent cross-sectional area of the flow, which is a variable parameter and depends on the exit angle of the flow from the nozzle (here turbine) and the turbine pressure ratio, π_T:

$$\pi_T = \frac{p_{ex}}{p_{gr}} \tag{5}$$

where p_{ex} is the exhaust gases pressure after the turbine at the exit point and p_{gr} is the pressure of gases at the exhaust gas receiver.

Eq. (2) is suitable for an isentropic flow. For a real case there are two different possibilities to calculate the flow rate. The first one, based on [69], considers the cross-sectional area of the flow as a function of the geometrical value of this area, A_T, and a correcting coefficient, a_T, which depends on the pressure ratio of the turbine, π_T, and the velocity ratio, $\frac{u}{c_s}$, as follows:

$$A_T^* = a_T A_T \tag{6}$$

$$a_T = a_T\left(\pi_T, \frac{u}{c_s}\right) \tag{7}$$

$$u = r_{T\,avg} \cdot \omega_{TC} \tag{8}$$

$$c_s = \left[\frac{2\kappa_T}{\kappa_T - 1} R_{gr} T_{gr} \left(1 - \pi_T^{\frac{\kappa_T - 1}{\kappa_T}} \right) \right]^{\frac{1}{2}} \tag{9}$$

In these relationships u stands for the turbine blade tip speed and c_s is the exhaust gases velocity under the isentropic condition and $r_{T\,avg}$ is the average radius of the turbine blades.

The second method, which is applicable in the absence of enough test results, considers A_T^* as a function of the same above-mentioned variables, which can be represented by the engine operating point, and then the equivalent cross-sectional area can be determined by using steady-state data for the given operating point.

Turbine energy balance

The power of the turbine is:

$$P_T = \dot{m}_5 \cdot (h_5 - h_{ex}) \tag{10}$$

where h stands for the enthalpy of the gases. Assuming the exhaust gases as semi-ideal gases, then this equation can be rewritten as follows:

$$P_T = \dot{m}_5 \cdot (c_{p5} \cdot T_5 - c_{pex} \cdot T_{ex}) \tag{11}$$

where c_p indicates the heat capacity at constant pressure. The isentropic temperature at the end of the expansion process after the turbine is::

$$T_{exs} = T_5 \cdot \pi_T^{\frac{\kappa_T - 1}{\kappa_T}} \tag{12}$$

By including the internal/adiabatic efficiency of the turbine for a real expansion process, this temperature in reality should be reduced as presented below:

$$T_{exs} = T_5 - \eta_T \cdot (T_5 - T_{exs}) \tag{13}$$

As a conclusion of the above equations, we get:

$$P_T = \dot{m}_5 \cdot \eta_T \cdot \frac{\kappa_T}{\kappa_T - 1} \cdot R_5 \cdot T_5 \cdot \left[1 - \pi_T^{\left(\frac{\kappa_T - 1}{\kappa_T}\right)} \right] \tag{14}$$

in which the gas constant and temperature at point 5 can be considered equal to the respected values for the exhaust gas receiver.

By excluding the heat exchange at the exhaust gas receiver, it is possible to assume that the temperature of the exhaust gases at point 5 and inside the exhaust gas receiver is the same. Therefore, the temperature of the exhaust gases at the outlet from the turbine is:

$$T_{ex} = T_{gr} - T_{gr}\,\eta_T \left[1 - \pi_t^{\left(\frac{k_t - 1}{k_t}\right)} \right] \tag{15}$$

In these calculations, it is assumed that a constant pressure exhaust gas receiver is applied, which today is a usual solution. For an impulse exhaust gas receiver, additionally a correction factor which has a higher value than one should be included, based on the experimental tests or using 3D CFD simulations.

Internal efficiency of the turbine

The static characteristic of the turbocharger is to be illustrated by the manufacturer. In this case, the turbocharger which consists of the compressor and turbine is considered as a unique element and its overall efficiency, η_{TC}, including the silencer pressure losses and the difference between the compressor and turbine mass flows, has been plotted against the pressure ratio of the compressor, π_C. This overall efficiency of the turbocharger, η_{TC}, can be approximated as a second-order polynomial function at steady states (see Fig. 2):

$$\eta_{TC} = \eta_T \cdot \eta_C = a_{TC} + b_{TC} \cdot \pi_C + c_{TC} \cdot \pi_C^{\,2} \tag{16}$$

and then the turbine efficiency can be determined:

$$\eta_T = \frac{\eta_{TC}}{\eta_C \cdot \eta_{TM}} \tag{17}$$

where η_C is the compressor's adiabatic efficiency and can be specified based on the compressor map (which will be discussed later) and η_{TM} is the mechanical efficiency of the turbine.

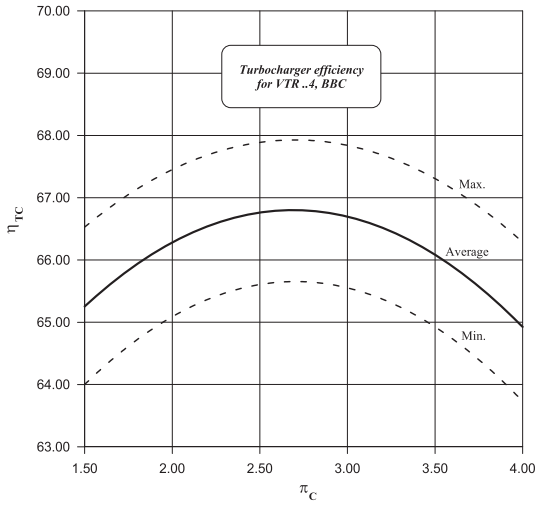

Fig. 2. Example of overall efficiency of the turbocharger [70]

Pressure ratio of the turbine

In order to specify π_T, it is necessary to express the exhaust gases pressure before and after the turbine, p_5 and p_{ex}. In many related references, p_{ex} has been considered equal to the ambient pressure, p_{at} and p_5 equal to the exhaust gas receiver pressure, p_{gr}. Although it is an alternative solution in the case of an absence of data, due to installation of the silencer and pressure drops in practice, there is a difference between these two sets of pressures

COMPRESSOR

Mass flow rate of air into the compressor

The mass flow rate of air through the compressor is a function of the angular velocity of the turbocharger shaft, ω_{TC}, the compressor pressure ratio, π_C, and the inlet air temperature:

$$\dot{m}_1 = \dot{m}_1(\omega_{TC}, \pi_C, T_0) \tag{18}$$

The most suitable way to determine the value of this function is by using the exact compressor map or similar scaled maps identified based on measurement or empirical relationships. The numerical modelling of the compressor map can be done using different approximation methods, supported by interpolation and extrapolation tools.
Ferenc, [15], has proposed the expression of the volumetric flow rate of the compressor, $\dot{v}_C(\omega_{TC}, \pi_C)$, by its approximation as a partial function as presented below

$$\dot{v}_C(\omega_{tc}) = \dot{v}_{C1}(\omega_{tc}) + \beta_{C1}(\omega_{tc}) \cdot \left[\beta_{C2}(\omega_{TC}) - \pi_c(\omega_{TC})\right]^{0.5} \tag{19}$$

hence

$$\dot{v}_{C1}(\omega_{TC}) = a_{C1} \cdot (\omega_{TC} - b_{C1}) \tag{20}$$

$$\beta_{C1}(\omega_{tc}) = a_{C2} \cdot (\omega_{TC} - b_{C2})^{-0.5} \tag{21}$$

$$\beta_{C2}(\omega_{TC}) = a_{C3} \cdot \omega_{TC}^{\,b_{C3}} + 1 \tag{22}$$

By the intersection of different values from the coBy the intersection of different values from the compressor map and considering three optional points of these characteristics, which have to satisfy Eq. (18), constant coefficients $a_{C\,i}$ and $b_{C\,i}$ can be determined. An example of a compressor map is presented in Fig. 3.

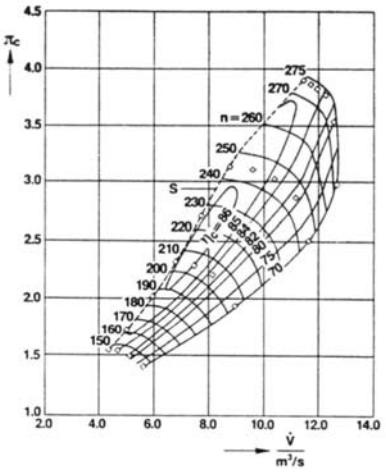

Fig. 3. Typical compressor characteristic (VTR ..4A) [70]

The compressor ratio pressure is known as the ratio of the total pressure to the ambient pressure:

$$\pi_c = \left(p_1 / p_{at}\right) \tag{23}$$

when

$$p_1 = p_{am} - \Delta p_{blr} + \Delta p_{clr} + p_{dyn} \tag{24}$$

and where p_{am} is the air pressure in the scavenging air manifold/receiver, p_{at} is the ambient pressure, Δp_{blr} is the pressure increase due to the application of auxiliary blowers (if installed), p_{clr} is the pressure drop in the charge air cooler and p_{dyn} is the dynamic pressure at the compressor outlet.
The auxiliary blowers (usually one or two) operate in parallel and in series with the compressor and they are placed after the charge air cooler. p_{am} can be calculated from the mass balance and energy balance for the scavenging air manifold/receiver. For easy calculation and to prevent any iterative process, Δp_{blr} and p_{dyn} can be defined in a highly simplified form [48] as follows:

$$\Delta p_{blr} = p_{blr\,0} - a_{blr}(p_{am} - p_{at})^2 \tag{25}$$

and

$$p_{dyn} = a_{dyn}(p_{am} - p_{at}) \tag{26}$$

where a_{blr} and a_{dyn} are constants that should be expressed based on experimental tests or the characteristics of the auxiliary blowers and the compressor. Constant a_{blr} should be taken to give zero pressure rise at approximately 30–50% power. At higher power levels the auxiliary blowers do not operate. The constant a_{dyn} is taken to give a typical dynamic pressure at the compressor outlet.

Compressor energy balance
The power of the compressor is:

$$P_C = \dot{m}_1 \cdot (h_1 - h_0) \tag{27}$$

where *h* stands for the enthalpy of the inlet air. Assuming the air as a semi-ideal gas, then:

$$P_C = \dot{m}_1 \cdot (c_{p1} \cdot T_1 - c_{p0} \cdot T_0) \tag{28}$$

where the parameters of point 0 can be assumed to be the same as the atmospheric parameters. The isentropic temperature at the end of the compression process after the compressor is:

$$T_{1s} = T_{at} \cdot \pi_C^{\frac{\kappa_T - 1}{\kappa_T}} \tag{29}$$

By including the internal/adiabatic efficiency of the compressor for a real compression process, this temperature in reality should be higher:

$$T_1 = \frac{1}{\eta_C} T_{at} \cdot \pi_C^{\frac{\kappa_T - 1}{\kappa_T}} \tag{30}$$

As a conclusion of the above equations, we get:

$$P_C = \frac{1}{\eta_C} \cdot \dot{m}_1 \cdot \frac{\kappa_C}{\kappa_C - 1} \cdot R_{at} \cdot T_{at} \cdot \left[1 - \pi_C^{\left(\frac{\kappa_C - 1}{\kappa_C}\right)}\right] \tag{31}$$

The internal/adiabatic efficiency of the compressor is a function of the angular velocity of the turbocharger shaft, ω_{TC}, the compressor pressure ratio, π_C, and the inlet air temperature:

$$\eta_C = \eta_C(\omega_{TC}, \pi_C, T_0) \tag{32}$$

The adiabatic efficiency of the compressor, η_C, can be tabulated according to the exact or scaled compressor map (see Fig. 3). For values which are not mentioned in the prepared table, cubic interpolation is recommended. The total efficiency of the compressor, when in addition the mechanical losses are assumed to be independent from ω_{TC} and π_C and therefore constant, can be obtained by multiplying the adiabatic efficiency and this mechanical efficiency.

ANGULAR VELOCITY OF TURBOCHARGER SHAFT

When the power of the compressor and turbine are defined, the dynamic of the angular velocity of the turbocharger shaft can be specified:

$$J_{TC}\,\dot{\omega}_{tc} = M_T - M_C - M_{TC\,loss} \tag{33}$$

where J_{TC} is the mass moment of inertia of the turbocharger rotating parts and shaft, and Mstands for the torque with lower indexes of T, C and TC_{loss} for the turbine, the compressor and the losses due to the heat dissipation and friction, respectively. The losses of the turbocharger, due to the high speed of the shaft, can be neglected or they may be adjusted based on the steady-state data by interpolation for different operating points.

CHARGE AIR COOLER

The reduction of the compressed air temperature at the inlet to the air manifold is achieved by a cooler. This is a function of the temperature of the available cooling medium and the effectiveness of the cooler, with the latter being expressed for an ideal gas as:

$$\begin{aligned}\varepsilon &= \frac{actual\ heat\ transfer}{Maximum\ possible\ heat\ transfer} \\ &= \frac{T_{in} - T_{out}}{T_{in} - T_w} \\ &= 1 - a_\varepsilon \cdot \dot{m}_1^{\,2}\end{aligned} \tag{34}$$

where T_{in} and T_{out} are the air temperature before and after the cooler, respectively and T_w is the temperature of the water inflow through the cooler. The effectiveness, ε, is expressed as a function of the mass flow rate of the inlet air. As for the effectiveness, the pressure drop imposed by the cooler on the air flowing through it is expressed as a function of the mass flow rate of the inlet air, [48]]:

$$\Delta p_{clr} = a^*_1 \cdot \dot{m}_c^{\,2} \frac{T_{in}}{p_{in}} \tag{35}$$

A linear relationship between the pressure drop in the cooler and the pressure of the scavenging air receiver can be considered:

$$\Delta\, p_{clr} = a_{clr}\,(p_1 - p_{at}) \tag{36}$$

Here, mass accumulation in the charge air cooler is not taken into account, when it is modelled through the scavenging air receiver/manifold.

Assuming that the cooling water temperature, T_w, is constant and the cooler efficiency, η_{clr}, is a function of the engine operating point (but constant at each point), the temperature of the compressed air after the cooler can be modelled as follows:

$$T_2 = T_1 - \eta_{clr} \cdot (T_1 - T_w) \tag{37}$$

MASS BALANCE EQUATION OF INLET AIR AND EXHAUST GASES RECEIVERS

The general equation of mass balance can be presented in the following simple form for each control volume:

$$\frac{dm}{dt} = \sum_{i=1}^{n} \dot{m}_i \tag{38}$$

Therefore, the continuity equations for the air mass flow rate through the intake air manifold/receiver (indicated by the lower index of *am*) and exhaust gases mass flow rate through the exhaust receiver (indicated by the lower index of *gr*) can be represented as follows, respectively:

$$V_{am} \cdot \overset{\circ}{\rho}_{ia} = \dot{m}_1 - \dot{m}_3 \tag{39}$$

$$V_{gr} \cdot \overset{\circ}{\rho}_{gr} = \dot{m}_4 - \dot{m}_5 \tag{40}$$

where V stands for the overall volume and ρ indicates the density.

ENERGY BALANCE EQUATION OF INLET AIR AND EXHAUST GASES RECEIVERS

The energy balance of the inlet air and exhaust gas receivers, as control volumes, expressed as the derivative of internal energy with respect to time, is as follows, [48]:

$$\frac{d(mu)}{dt} = \frac{dQ}{dt} - p\frac{dV}{dt} + \sum_{i=1}^{n} h_i \cdot \dot{m}_i \tag{41}$$

where *m, u, p, V, Q* and h are the mass, specific internal energy, pressure, volume, heat and specific enthalpy, respectively. The positive sign of the energy and mass transfer in this general equation and the further equations indicates the flow direction into the receivers.

The derivative of the internal energy is:

$$\frac{d(mu)}{dt} = m\frac{du}{dt} + u\frac{dm}{dt} \tag{42}$$

The derivative of the specific internal energy can be expressed through the temperature derivative of the fuel-to-air (or equivalence) ratio of the exhaust gas in the control volume. The internal energy is a function of the temperature and equivalence ratio:

$$\frac{du}{dt} = \frac{\partial u}{\partial T}\frac{dT}{dt} + \frac{\partial u}{\partial F}\frac{dF}{dt} \tag{43}$$

where the fuel-to-air ratio, f, is related to the equivalence ratio of exhaust gas, F, as

$$F = \frac{f}{f_{sto}} \tag{44}$$

and f_{sto} is the stoichiometric fuel-to-air ratio.

The partial derivative of internal energy with respect to temperature is the specific heat in constant volume, c_v. It can be expressed through the specific heat at constant pressure and gas constant:

$$\frac{\partial u}{\partial T} = c_v = c_p - R \tag{45}$$

hence c_p is the specific heat in constant pressure and R is the universal gas constant (8.4134 kJ/kmol K).

The partial derivative of internal energy with respect to the equivalence ratio of exhaust gas is:

$$\frac{\partial u}{\partial F} = u - u_{at} \tag{46}$$

The derivative of the equivalence ratio with respect to time can be expressed as:

$$\begin{cases} \dfrac{dF}{dt} = \dfrac{F1}{m}\left(\dfrac{F1}{f_{sto}}\dfrac{dm_{fb}}{dt} - F\dfrac{dm}{dt}\right) \\ F1 = 1 + F f_{sto} \end{cases} \tag{47}$$

By solving Eq. (44) with respect to the derivative of temperature and by using Eqs (42) and (43), the equation of the energy balance for a one-zero control volume can be expressed as:

$$\frac{dT}{dt} = \left[\frac{1}{m}\left(\sum\frac{dQ}{dt} + \sum h\frac{dm}{dt} - p\frac{dV}{dt} - u\frac{dm}{dt}\right) - \frac{\partial u}{\partial F}\frac{dF}{dt}\right]\frac{1}{\partial u/\partial T} \tag{48}$$

Considering that there is no change of the fuel-to-air ratio in the inlet air and exhaust gas receiver, $(dF/dt) = 0$, no change of the overall volume, $(dV/dt) = 0$, neglecting the heat exchange between the receivers' wall and the surround, $(dQ/dt) = 0$, and having that $h = c_p \cdot T$ $u = c_v \cdot T$, then the temperature time variation for each of these receivers can be rewritten as given below:

- For the intake air manifold/receiver:

$$\frac{dT_{am}}{dt} = \frac{1}{m_{am}}\left[\left(\frac{c_{p\,2}}{c_{v\,am}}\right)\cdot\dot{m}_2\cdot T_2 - \left(\frac{c_{p\,am}}{c_{v\,am}}\right)\cdot\dot{m}_3\cdot T_3 - T_{am}\cdot\dot{m}_{am}\right] \tag{49}$$

- For the exhaust gas receiver:

$$\frac{dT_{gr}}{dt} = \frac{1}{m_{gr}}\left[\left(\frac{c_{p\,4}}{c_{v\,gr}}\right)\cdot\dot{m}_4\cdot T_4 - \left(\frac{c_{p\,gr}}{c_{v\,gr}}\right)\cdot\dot{m}_5\cdot T_5 - T_{gr}\cdot\dot{m}_{gr}\right] \tag{50}$$

The mass flow rate at point 4, after the engine cylinders, i.e., $\dot{m}_4$, should be determined as follows:

$$\dot{m}_4 = \dot{m}_3 + \dot{m}_f \tag{51}$$

where $\dot{m}_f$ is the fuel mass flow rate into the engine cylinders. The pressure of the intake air and exhaust gases in these receivers can be determined as follows:

- For the intake air manifold/receiver:

$$p_{am} = \frac{m_{am}\cdot R_{am}\cdot T_{am}}{V_{am}} \tag{52}$$

- For the exhaust gas receiver:

$$p_{gr} = \frac{m_{gr}\cdot R_{gr}\cdot T_{gr}}{V_{gr}} \tag{53}$$

THE ENGINE CYLINDERS AND COMBUSTION PROCESS

For a mean-value model, it is assumed that all cylinders of the engine are shaping one block of the model. This means that instead of modelling each cylinder individually and then combining them to get the overall performance of the engine cylinders, the mean values of the variables of all the included cylinders are taken into account. The thermodynamic phases, i.e., closed cycle periods with and without combustion, exhaust or blow-down period, and valve overlap or scavenging period, as well as the inlet period, are not modelled separately. The heat exchange is considered and combustion efficiency is determined, but again as an overall process. In this case, the inputs to the cylinders are the charge air coming from the intake air manifold/receiver and the fuel mass flow rate. The outputs are the mass flow rate of the exhaust gases, engine torque, M_E, and engine shaft angular velocity, ω. Assuming that the power transmission from the cylinders to the engine shaft occurred immediately, without any time delay, then the dynamics of the engine shaft can be separately modelled by including all other moments of mass inertia related to other components of the engine and propeller shaft. Another important consideration is related to the influence of torsional vibrations of the crankshaft. These can be omitted here, because the time constant of the turbocharger and its components is much greater than the time constants determined for the dynamics of the crankshaft and engine shaft.

Mass flow rate through the engine

Similar to the model of the exhaust gases mass flow rate through the turbine of the turbocharger, here the mass flow rate of the medium through the engine can be modelled based on the flow function of a nozzle with an equivalent flow cross-sectional area. Therefore, the flow rate of the air and exhaust gases depends on the engine (cylinders) pressure ratio and it can represented as follows:

$$\dot{m}_3 = A^*_{cyl} \cdot \psi_{cyl}(\pi_{cyl}) \cdot \sqrt{p_3 \cdot \rho_3} \tag{54}$$

where the flow function should be calculated as was mentioned in Eqs. (3) and (4) with the cylinders pressure ratio defined as follows:

$$\pi_{cyl} = \frac{p_{gr}}{P_{am}} \tag{55}$$

The equivalent cross-sectional area of the flow, A^*_{cyl}, can be assumed as a constant at a given operating point in steady states and derived from the experimental tests or calculated from the steady state characteristics delivered by the manufacturer. In unsteady states, its value can be interpolated for a quasi-steady approach. The values of the adiabatic exponent as a function of temperature, depending on the specific heats at constant pressure and constant volume for a given fuel-to-air ratio and temperature, can be determined as presented in Appendix A.

It should be noted that a part of the inlet air to the cylinders is used for blowing-down the cylinders and will not be part of the combustion process (Fig. 4).

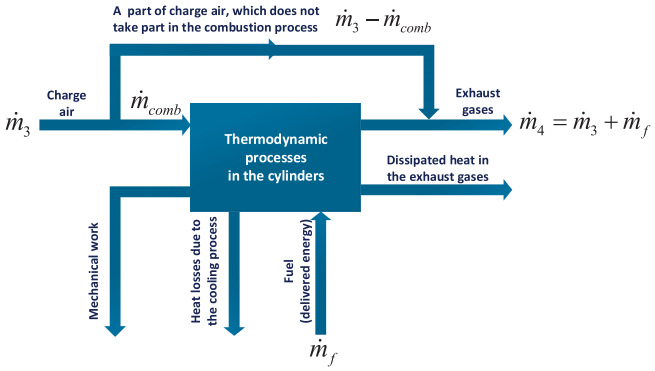

Fig. 4. Schematic diagram of mass flow and energy distribution in the engine cylinders

The fraction of air that takes part in the combustion process, $\dot{m}_{comb}$, can be determined by reduction of the theoretically calculated air consumed by the engine, $\dot{m}_{combt}$, using an efficiency index that applies the degree of filling the cylinders in reality in comparison to the theoretical value:

$$\dot{m}_{comb} = \eta_{cyl} \cdot \dot{m}_{combt} \tag{56}$$

where this efficiency, η_{cyl}, is the relation of the charge air supplied to the cylinders to the overall stroke volume of the cylinders. $\dot{m}_{combt}$ can be determined as followss:

$$\dot{m}_{combt} = \frac{\omega}{2\pi} \cdot V_{cyl} \cdot \rho_3 \cdot Z \tag{57}$$

in which V_{cyl} is the stroke volume of one cylinder, measured from the bottom dead centre to the upper dead centre and Z is the number of cylinders. The density at point 3 can be considered as the air density in the intake air manifold/receiver, i.e.:

$$\rho_3 \approx \frac{R_{am} T_{am}}{p_{am}} \tag{58}$$

Based on [8], the filling efficiency is an inverse function of the blow-down coefficient, λ_b. This coefficient has been defined in national or international norms. For example [71] defines this efficiency as the ratio of the delivered mass of air to a cylinder within one working cycle to the trapped air mass in the cylinder:

$$\lambda_b \approx \frac{\dot{m}_3}{\dot{m}_{combt}} \tag{59}$$

hence:

$$\eta_{fill} = 1 - \exp\left(-k_b \cdot \lambda_b\right) \tag{60}$$

in which k_b is a constant that can be identified experimentally or determined based on the engine operational performance in steady states.

By considering the last five equations, $\dot{m}_{comb}$ can be specified as follows:

$$\dot{m}_{comb} = \frac{\omega}{2\pi} \cdot Z \cdot V_{cyl} \cdot \frac{R_{am} T_{am}}{p_{am}} \cdot \left[1 - \exp\left(-k_b \cdot \lambda_b\right)\right] \tag{61}$$

where:

$$\lambda_b = \frac{2\pi \cdot \dot{m}_3 \cdot R_{am} \cdot T_{am}}{\omega \cdot Z \cdot V_{cyl}} \tag{62}$$

The indicated engine power

Taking into account the air mass flow rate that is to be used for the combustion process and having the fuel flow rate into the cylinders, then it is possible to calculate the indicated engine power:

$$P_E = \eta_E \cdot \dot{m}_f \cdot q_f \tag{63}$$

where P_E is the engine indicated power, η_E is the thermal efficiency of the engine, and q_f is the fuel low heat calorific value. In reality, the engine thermal efficiency is a function of different variables such as the inlet air flow rate, fuel flow rate, heat exchange of the cylinder walls, engine angular velocity, etc. However, it is common practice to consider it as a function of the engine's excess air coefficient, λ. This coefficient is defined as follows:

$$\lambda = \frac{\dot{m}_{comb}}{\lambda_t \cdot \dot{m}_f} \tag{64}$$

where λ_t is the required theoretical air excess coefficient calculated for stoichiometric chemical reaction of the combustion process.

To calculate the engine thermal efficiency in steady state, when the excessive air coefficient is known, the following approximation can be taken into account, [17]:

$$\eta_E(\overline{\omega}, \lambda) = \begin{cases} \eta_{EM}(\overline{\omega}) & ; \quad \lambda \geq \lambda_M \\ \eta_{EM}(\overline{\omega}) - \beta_E \cdot \left[\lambda_M(\overline{\omega}) - \lambda\right]^{\alpha_E} & ; \quad \lambda < \lambda_M \end{cases} \tag{65}$$

Hence:

$$\eta_{EM}(\overline{\omega}) = \begin{cases} a_{E1}.\overline{\omega} + b_{E1} & ; \quad \overline{\omega} \leq \Omega \\ a_{E2}.\overline{\omega} + b_{E2} & ; \quad \overline{\omega} > \Omega \end{cases} \tag{66}$$

$$\beta_E(\overline{\omega}) = \begin{cases} a_{E3}.\overline{\omega} + b_{E3} & ; \quad \overline{\omega} \leq \Omega \\ a_{E4}.\overline{\omega} + b_{E4} & ; \quad \overline{\omega} > \Omega \end{cases} \tag{67}$$

$$\lambda_M(\overline{\omega}) = \begin{cases} a_{E5}.\overline{\omega} + b_{E5} & ; \quad \overline{\omega} \leq \Omega \\ a_{E6}.\overline{\omega} + b_{E6} & ; \quad \overline{\omega} > \Omega \end{cases} \tag{68}$$

where α_E, a_{Ei}, b_{Ei} (i = 1 to 6) and Ω are constants, expressed by the experimental tests or determined based on the steady-state performances, and index *M* illustrates the optimal value of each parameter at the specified angular velocity ω. The symbol $\overline{\omega}$ indicates the non-dimensional value of the engine angular velocity in relation to its maximum value.

In steady state the temperature field of the combustion chamber walls is stabilised and can be presented as a function of the angular velocity of the engine and partial excessive air coefficient. However, when a rapid load changing happens, the temperature field of the combustion chamber walls does not vary in the same way as ω and λ change. Therefore, the engine's thermal efficiency calculated for the steady state does not coincide with the dynamic test results. As a conclusion, in transient conditions the engine's thermal efficiency differs from its value in the steady state. To overcome these difficulties, a highly simplified linear model can be applied as follows:

$$\Delta\eta_E = k_{\eta_E} \cdot \Delta\lambda \tag{69}$$

and the constant k_{η_E} can be determined for each operating point at steady state and then interpolated for unsteady states. Additionally, when the engine steady-state performances are given by the manufacturer, then for a given heat calorific value of the fuel, and by knowing the engine power, the engine's thermal efficiency at each operating point can be calculated.

Combustion and the exhaust gases parameters

The energy balance equation of the cylinders can be represented as follows:

$$\dot{h}_{air} + \dot{q}_{comb} = \dot{q}_{loss} + P_E + \dot{h}_{ex\_gas} \tag{70}$$

where $\dot{h}_{air}$ is the rate of enthalpy of the charge air used for combustion, $\dot{q}_{comb}$ is the rate of heat release during combustion, $\dot{q}_{loss}$ is the rate of heat losses dissipated because of the cooling process, and $\dot{h}_{ex\_gas}$ is the rate of enthalpy of exhaust gases after combustion. The enthalpy of the supplied fuel is omitted here because its value in comparison to other elements of the equation is low and negligible. The elements of Eq. (70) can be determined as follows:

$$\dot{h}_{air\_comb} = \dot{m}_{comb} \cdot c_{p_3} \cdot T_3 \tag{71}$$

$$\dot{h}_{ex\_gas} = (\dot{m}_{comb} + \dot{m}_f) \cdot c_{p_4} \cdot T_{comb} \tag{72}$$

$$\dot{q}_{comb} = \dot{m}_f \cdot q_f \tag{73}$$

$$\dot{q}_{loss} = k_{loss} \cdot \dot{q}_{comb} \tag{74}$$

where T_{comb} is the temperature of that part of the exhaust gases which are produced during the combustion process. The last equation indicates that the rate of heat losses because of cooling is a part of the rate of heat released in the cylinders, and the coefficient of k_{loss} is constant for each operating point at the steady states. This coefficient can be measured indirectly or determined using the steady- state performance.

By substituting the last four equations in Eq. (71), the temperature of that part of the exhaust gases which are produced during the combustion process can be determined:

$$T_{comb} = \frac{q_f \cdot \dot{m}_f \cdot (1 - k_{loss}) - P_E}{(\dot{m}_{comb} + \dot{m}_f) \cdot c_{p_4}} + T_{am} \cdot \frac{\dot{m}_{comb}}{\dot{m}_{comb} + \dot{m}_f} \cdot \frac{c_{p_{am}}}{c_{p_4}} \tag{75}$$

where the thermodynamic parameters of point 3 are assumed to be the same as in the intake air manifold/receiver.

The temperature of the exhaust gases flowing to the exhaust gases receiver at point 4 is a result of mixing of the exhaust gases produced during the combustion process and the part of the charge air that did not participate in the combustion process (Fig. 5).

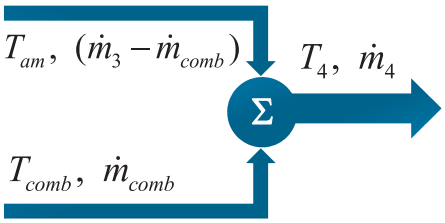

Fig. 5. The schematic diagram of the exhaust gases outflow parameters from the cylinders

The energy balance equation can then be written as follows:

$$T_4 \cdot \dot{m}_4 \cdot c_{p_4} = T_{am} \cdot (\dot{m}_3 - \dot{m}_{comb}) \cdot c_{p_{am}} + T_{comb} \cdot \dot{m}_{comb} \cdot c_{p_{comb}} \tag{76}$$

which in turn gives the following relationship for the temperature at point 4:

$$T_4 = T_{am} \cdot \frac{c_{p_3}}{c_{p_4}} \cdot \frac{\dot{m}_3 - \dot{m}_{comb}}{\dot{m}_4} + T_{comb} \cdot \frac{\dot{m}_{comb}}{\dot{m}_4} \cdot \frac{c_{p_{comb}}}{c_{p_4}} \tag{77}$$

where the heat capacity at constant pressure is to be considered the same for point 3 and the intake air manifold/receiver.

THE ANGULAR VELOCITY OF THE ENGINE SHAFT

The shafting system is modelled as a rigid body. The derivative of propeller shaft angular velocity is

$$(J_E + J_P + J_S) \cdot \dot{\omega} = M_E - (M_P + M_{loss}) \tag{78}$$

where ω is the angular velocity of the engine shaft, M indicates the torque, J stands for the mass moment of inertia, and lower indexes *E, P, S* and loss indicate the engine, propeller, power transmission shaft and its components, and mechanical losses, respectively.

Mechanical losses are caused by the engine reciprocating motion, rotation of the connected parts and engine-mounted and engine-driven auxiliaries. However, the main attempt in this case, at least for simulation of the dynamic behaviour of the diesel engine as a prime mover, is concentrated only on the engine, singularly. Potentially, the best method for evaluating the mechanical losses in the form of friction is to evaluate the indicated power output from an accurate cylinder pressure diagram and to subtract the measured brake power output. To do this carefully, it would be better to motor the engine, electrically. Mechanical losses can be presented in the form of either torque or mean effective pressure losses. It is recognised that the mechanical losses depend on the engine angular velocity (or mean piston speed) and the peak cylinders pressure [72]. Although it affects the bearing loads, this effect is almost negligible. Therefore, the proposed mechanical losses in the form of the mean effective pressure can be presented as follows:

$$M_{loss} = a_l + b_l\ p_{peak}^{\ c_l} + d_l \left(\omega - \omega_{\min}\right)^{e_l} \tag{79}$$

where P_{peak} is the peak pressure of the cylinder, ω_{min} is the minimum required angular velocity of the engine for continuous running (minimum permissible velocity), and a_l, b_l, c_l, d_l and e_l are constants for losses calculation. If the second term of the above equation is not negligible, c_l can be considered equal to one [41]. e_l depends on the engine type and is between zero and one for a low-speed diesel engine and from one to two for a medium-speed diesel engine. Other constants should be verified based on the experimental data or steady-state performance for a given operating point.

In the present study the effect of pressure is omitted, and M_{loss} is formulated as follows:

$$M_{loss} = a_l + d_l \left(\omega - \omega_{\min}\right) \tag{80}$$

Hence, for modelling of the diesel engine, the problem of determining the propeller torque is not discussed here and for the sake of simplicity it is modelled as a second-order function of the engine shaft angular velocity:

$$M_P = k_P \cdot \omega^2 \tag{81}$$

where k_P is a constant for a given operating point, which can be determined as follows:

$$k_P = \frac{N_E}{\omega^3} \tag{82}$$

NO_x EMISSION

The most important parameter affecting the generation of NO_x is the fuel-to-air equivalence ratio [73]. By considering the Zeldovich mechanism of NO_x generation:

$$O + N_2 \rightarrow NO + N \tag{83}$$

$$N + O_2 \rightarrow NO + O \tag{84}$$

$$N + OH \rightarrow NO + H \tag{85}$$

and based on [73] the rate of formation of NO can be simplified as follows:

$$\frac{d[NO]}{dt} = \frac{6 \cdot 10^{16}}{\sqrt{T}_b} \exp\left(\frac{-69090}{T_{comb}}\right) [O_2]_e^{\ 1/2} [N_2]_e$$

where [ ] denotes species concentrations in [mole/m^3] and subscript $_e$ stands for the equilibrium state and can be determined for a specific component of the intake air to the compressor. In the case of NO_2, it is shown that for the majority of marine diesel engines its approximate rate of

formation is usually around 10% of the rate of formation of NO [73].

THE OVERALL MODEL ALGORITHM

The considered state variables are:

1. Mass of air in the air inlet manifold/receiver, m_{am},
2. Temperature of air in the air inlet manifold/receiver, T_{am},
3. Mass of exhaust gases in the exhaust gases receiver, m_{gr},
4. Temperature of the exhaust gases in the exhaust gas receiver, T_{gr},
5. Angular velocity of the turbocharger shaft, ω_{TC},
6. Angular velocity of the power transmission shaft, ω,
7. Rate of formation of NO (and NO_2)

After providing the initial values of the state variables and the mass flow rate of the fuel based on the selected operating steady point, the overall algorithm of the model for calculating the gradient of state variables is as follows:

1. Read the model parameters;
2. Determine or read the thermo-physical properties of the inlet air and the exhaust gases at different model points (see Appendix A);
3. Calculate the turbine variables:
   i. Mass flow rate of the exhaust gases before the turbine, $\dot{m}_5$, Eq. (2),
   ii. The power of the turbine, P_T.
4. Calculate the compressor variables:
   i. The pressure after the compressor,p_1 , as well as the compressor pressure ratio,
   ii. The volumetric flow rate and the compressor efficiency based on the similar compressor map,
   iii. Read the correction factor of the compressor efficiency and calculate the scaled compressor efficiency, as well as the mass flow rate,
   iv. The scaled compressor power.
5. Calculate the charge air cooler variables:
   i. The temperature before the charge air cooler, T_1 ,
   ii. The temperature after the charge air cooler, T_2,
6. Calculate the variables of the engine cylinders:
   i. The mass flow rate of the air into the engine cylinders, $\dot{m}_3$,
   ii. The mass flow rate of the exhaust gases after the engine cylinders, $\dot{m}_4$,
   iii. The mass flow rate of that part of air that takes place in the combustion process, $\dot{m}_{comb}$,
   iv. The temperature of that part of the exhaust gases that are produced during the combustion process, T_{comb}
   v. The temperature of the exhaust gases after the engine cylinders, T_4,
   vi. The temperature of the exhaust gases after the turbine,.T_{exit}
7. Calculate the propeller and engine torques.
8. Determine the gradients of state variables.

SETTING UP THE MODEL PARAMETERS

Generally, the model parameters should be set based on the experimental tests, empirical formulae or the available data delivered by the engine manufacturer. Here, mainly the latter is used. These are data that are publicly available. The assumption is that no additional protected or confidential data are required to set up the necessary parameters. The data should be taken from the engine project guides, turbocharger catalogues specified for the steady-state operational conditions. The widely available drawings of the engine and its components are necessary too.

The following part describes the procedure for determining or identifying the model parameters, step by step.

A. Preparing the initial data

1. Read the geometry of the engine, its cylinders, intake air manifold/receiver and exhaust gas receiver. These data should include at least the volume of the intake air manifold/receiver, the volume of the exhaust gases receiver, diameter of the cylinders, and the engine stroke. The number of cylinders should be given too. Calculate the overall volume of the cylinders:

$$V_{cyl} = \frac{\pi}{4} \cdot D_{cyl}{}^2 \cdot S_{cyl} \cdot Z_{cyl} \tag{86}$$

   where D_{cyl}, S_{cyl} and Z_{cyl} stand for the diameter, stroke and number of cylinders, respectively.
2. Read the table of steady-state values of the engine variables at each operating point, which are given as a percent of the Service Maximum Continuous Rating. The variables should include at least the engine power, rate of rotation of the engine shaft, specific fuel consumption, exhaust gas amount and their temperature at the exit of the turbine.
3. Read the turbocharger parameters including at least the turbocharger efficiency and average radius of the compressor wheel. Additionally, having the compressor map may reduce the number of iterations in the further steps.
4. Specify the ambient conditions including pressure and temperature, and if possible the humidity.

B. Calculating the initial parameters

1. Having the efficiency of the turbocharger and the compressor map, calculate the turbine efficiency using Eq. (17). If the compressor map is not available, set the turbine efficiency between 0.85 and 0.95 respectively for SMCR between 10% and 100% and apply a linear regression. These values can be adjusted and improved for the applied turbocharger in the next trial and error step.
2. Assume the density of the exhaust gases receiver. The corresponding values for 10% of SMCR up to 100% can be linearly distributed from 1.25 kg/m^3 to 1.30 kg/m^3, respectively, for the first iteration. Again, they can be improved and correctly adjusted for the given engine in the next iterations.

3. Prepare a look-up table and read the values of the compressor efficiency, η_C, for different engine operating points at steady states. If the compressor map for the given engine is not available, select another but similar (as far as possible) compressor and then define a correction factor, *CF*, for the compressor efficiency:

$$\eta_C = CF \cdot \eta_{C_S} \tag{87}$$

where η_{C_S} stands for the similar compressor efficiency. At the beginning, the value of the correction factor can be set as equal for all operating points and it will then be modified in the further steps or iterations.

4. For the specified ambient conditions determine the parameters of the inlet air, i.e., the specific heats at constant pressure, $c_{p_{at}}$, and at the constant volume, $c_{v_{at}}$, adiabatic exponent, κ_{at}, and gas constant R_{at}; see Appendix A.
5. Select a charge air cooler and read the cooler efficiency. This can be considered as a constant value. For the specified ambient conditions set the temperature of the cooling water, T_W.
6. For the applied fuel, read the low heat calorific value of the fuel, q_f.

C. The iteration loop

For each operating point, i.e., %SMCR, which is hereafter indicated by *OP*, follow the procedure given below.

1. Having the temperature of the outflowing exhaust gases from the turbine, T_{ex}, (delivered by the engine manufacturer), use the following iteration method to calculate the temperature of the exhaust gases in the exhaust gases receiver:
   i. Inputs: T_{ex}, p_{at}, η_T, ρ_{gr}, $\dot{m}_f$ and $\dot{m}_{ex}$;
   ii. Calculate the fuel-to-air ratio, *f*:

$$f = \frac{\dot{m}_f}{\dot{m}_{ex} - \dot{m}_f} \tag{88}$$

   iii. Set $\Delta = 200$, (as an example, it should be a high enough value);
   iv. Set $T_{g1} = T_{ex} + \Delta$
   v. While $\delta > tol$ (for example: $tol = 0.01$)
      a. Calculate the adiabatic exponent, gas constant, pressure of the exhaust gases and turbine pressure ratio for temperature equal to T_{g1} and for the given fuel-to-air ratio (see Appendix A);
      b. Calculate the temperature of the outflowing exhaust gases considering $T_{g1} = T_5$:

$$T_{ex1} = T_{g1} - T_{g1} \cdot \eta_T \cdot \left(1 - \pi_T^{\frac{\kappa_{g1}-1}{\kappa_{g1}}}\right) \tag{89}$$

      c. Determine δ: $\delta = |T_{ex} - T_{ex1}|$
      d. Set $T_{g1} = (T_{g1} - \varepsilon)$, where ε stands for the minimum temperature increment, e.g. 0.002;

   End

   vi. Set: $T_{gr} = T_{g1}$.

2. Consider the temperature at point 5 equal to the temperature of the exhaust gases at the exhaust gas receiver: $T_5 = T_{gr}$.
3. Calculate the adiabatic exponent, gas constant, pressure of the exhaust gases at the exhaust gas receiver and the turbine pressure ratio for the temperature equal to T_5 and for the given fuel-to-air ratio at the specified *OP* (see Appendix A);
4. Calculate the mass flow rate through the turbine at point 5, $\dot{m}_5$, Eqs. (2), (3) and (4);
5. Calculate the power delivered by the turbine, P_T, Eq. (14);
6. Calculate the mass of exhaust gases at the exhaust gases receiver:

$$m_{gr} = \frac{p_{gr} \cdot V_{gr}}{R_{gr} \cdot T_5} \tag{90}$$

7. Set the pressure of the intake air manifold/receiver, p_{am}, considering that it should be higher than the pressure of the exhaust gases in the exhaust gas receiver by approximately 3% to 15% for the lowest and the highest operating point, respectively. This is an empirical result calculated for a set of selected large-stroke low-speed marine diesel engines. Here, a second order polynomial approximation is preferred, but a linear approximation should be enough too.
8. Calculate the compressor pressure ratio, π_C, Eqs. (23) to (26);
9. Having the real or similar compressor map, set and determine the compressor tip speed (the linear velocity of the compressor wheel tip) as a first- or second-order polynomial function of the *OP*, when the minimum value is considered for the lowest operating point;
10. Having the compressor tip speed, calculate the rate of revolution of the turbocharger shaft, ω_{TC};
11. Read the volumetric flow rate of the compressed air and the efficiency of the compressor from the applied or similar compressor map, $\dot{v}_{Cs}$;
12. Using the volumetric flow rate of the real or similar compressor, calculate the mass flow rate of the compressed air, $\dot{m}_{Cs}$ (see also Eq. (19)):

$$\dot{m}_{Cs} = \rho_{at} \cdot \dot{v}_{Cs} \tag{91}$$

13. Calculate the mass flow rate of the air after the compressor as follows:

$$\dot{m}_1 = \dot{m}_5 - \dot{m}_f \tag{92}$$

14. Determine the compressor efficiency by including the correction factor, see Eq. (87);
15. Calculate the initial power required by the compressor, Eq. (31);
16. Modify the correction factor as follows:

$$CF = \frac{\dot{m}_1}{\dot{m}_{Cs}} \tag{93}$$

17. Having the new correction factor, calculate the modified value of the mass flow rate of the air after the compressor by multiplying the value obtained from Eq. (91) to the correction factor;
18. Again calculate the power required by the compressor, Eq. (31),using the modified mass flow rate of the air after the compressor and consider this power as the compressor power for further calculations;
19. Calculate the temperature after the compressor, T_1, using Eq. (30);
20. Having the temperature of the air after the compressor, it is now possible to estimate the temperature after the charge air cooler, T_2, using Eq. (37). Additionally, for the sake of simplification and because of the relatively low temperature gradient in the inlet air manifold/receiver walls, the heat exchange can be neglected and the temperature of the inlet air to the engine cylinders, T_3, can be assumed equal to T_2, and then the thermodynamic parameters of the air at this temperature can be specified (Appendix A);
21. For further calculations, a simplification can be applied by considering the mass flow rate of the air after the charge air cooler, $\dot{m}_2$, equal to the mass flow rate after the compressor (no losses). This mass flow rate can also be applied as the mass flow rate of the air into the engine cylinders, $\dot{m}_3$. Additionally, the mass flow rate of the exhaust gases after the cylinders, $\dot{m}_4$, should be equal to the mass flow rate of the inlet air into the engine cylinders added to the mass flow rate of the fuel, which is equal to the mass flow rate after the exhaust gas receiver into the turbine, $\dot{m}_5$.
22. Again, by neglecting the heat exchange in the exhaust gas receiver walls, the temperature of the exhaust gases after the engine cylinders can be considered equal to the temperature of the exhaust gases after the exhaust gas receiver, i.e., $T_4 = T_5$;
23. Calculate the mass flow rate of the exhaust gases through the engine cylinders using Eq. (54) when applying Eq. (55), and the gas parameters are set for point 3 (before the engine cylinders);
24. Calculate the blow-down coefficient, λ_b, based on Eq. (62);
25. To be able to calculate k_b (the constant that should be specified for determining the combustion efficiency, see Eq. (60)), select an initial value for the filling efficiency, for instance 0.9 for all operating points. This value will be corrected for each operating point in the next loops. Then k_b is calculated as follows:

$$k_b = -\ln\left(\frac{1-\eta_{fill}}{\lambda_b}\right) \tag{94}$$

26. Calculate the part of the air that takes part in the combustion process, $\dot{m}_{comb}$, using Eq. (61);
27. Calculate the engine power by applying Eq. (63);
28. To find k_{loss} , which is necessary for calculating the temperature of the part of the exhaust gases that is produced during the combustion process, T_{comb}, (see Eq.(75)), apply the following loop for each operating point:
    i. Set: k_{loss} =0; δ=0;
    ii. While $\delta \geq 0.001$ (note: 0.001 is a tolerance for accuracy of the temperature)
        a. Calculate T_{comb} by using Eq. (75)
        b. Calculate the thermodynamic properties of the exhaust gases at the temperature of T_{comb} and by considering the fuel-to-air ratio of the gases (Appendix A)
        c. Calculate the nominal temperature of the exhaust gases after the engine cylinders at point 4, T_{40}, using Eq. (77);
        d. Calculate $\delta = T_{40} - T_4$
        e. Set $k_{loss} = k_{loss}$ + 1e-6
    iii. End.
29. Determine the current mass of air in the air inlet manifold/receiver.

D. Checking process before the next loop

At the end of each iteration loop, it is necessary to check whether the calculated or adjusted parameters satisfy the basic equations in relation to each operating point at steady states. These basic equations and checking process are given below. The hierarchy of checking should be respected, e.g., it is necessary to satisfy Eq. (95) and then in the next loops satisfy Eq. (96), etc.

1. $$P_C = P_T \tag{95}$$

If $P_C > P_T$, then the turbine efficiency, η_T, and/or exhaust gases density, ρ_{gr}, are candidates that should be increased and vice versa. The increment should be considered at a low level, for example 1e-7, for each.

2. $$\dot{m}_1 = \dot{m}_3 \tag{96}$$

If m $\dot{m}_3 > \dot{m}_1$, then the correction factor for the compressor efficiency, *CF*, (see Eq. (87)) can be increased and vice versa. The increment again should be at a low level, e.g. 1e-6.

3. $$\begin{aligned} \dot{m}_4 &= \dot{m}_5 \\ &= \dot{m}_3 + \dot{m}_f \end{aligned} \tag{97}$$

Checking this equation, it is necessary to take into account also how the calculated exhaust gas temperature is matched to the given temperature by the manufacturers. This condition is affected by Eq. (75) and the coefficients included in this equation. The latter can be adjusted by fitting the filling efficiency to the adequate value.

4. $$P_E = P_P \tag{98}$$

If $P_P \neq P_P$ then k_P in Eq. (82) should be adequately corrected.

CASE STUDY

The case selected for modelling and analysing is a MAN-B&W 8S65ME-C8.5 low-speed diesel engine. The Service Maximum Continuous Rating (SMCR) for the considered ship is set at 19433 kW @ 92.8 rpm.

The steady-state performance of the engine and necessary engine drawings can be taken from the Computerized Engine Application System (CEAS). The general features of the engine are given in Table 1. The engine performance at steady states at different operating points from 10% to 100% of SMCR is given in Table 2 and important variables are illustrated in Fig. 6.

Table 1. The general features of the selected engine (MAN-B&W 8S65ME-C8.5), [74, 75]

IMO Tier Regulation	Tier II
Catalogue	Official catalogue
Fuel Injection Concept	DI (Diesel)
Engine Category	ME
Turbocharger Efficiency	High
SFOC Optimized Load Range	High load
Fuel Sulphur Content	Low sulphur (0.5%)
Scrubber Installation	Installed
Total Brake Pressure of Exhaust System (Tier II Total Back Pressure [mbar]	30
SMCR Speed [rpm]	92.8
SMCR Power	9433 [kW]
Normal Cont. Rating (NCR)	100
Engine Cooling System	Fresh water
Custom Ambient Condition	ISO
Propeller Type	FPP
Hydraulic System Oil	Common
Hydraulic Power Supply	Mechanical
Turbocharger Lubrication	Common
Hydraulic Control System	Unified
Cylinder Lubrication	MAN B&W Alpha
Turbocharger	MAN B&W High Eff. TCA88
LCV for Fuel Oil [kJ/kg]	42707
Steam Pressure [bar]	7

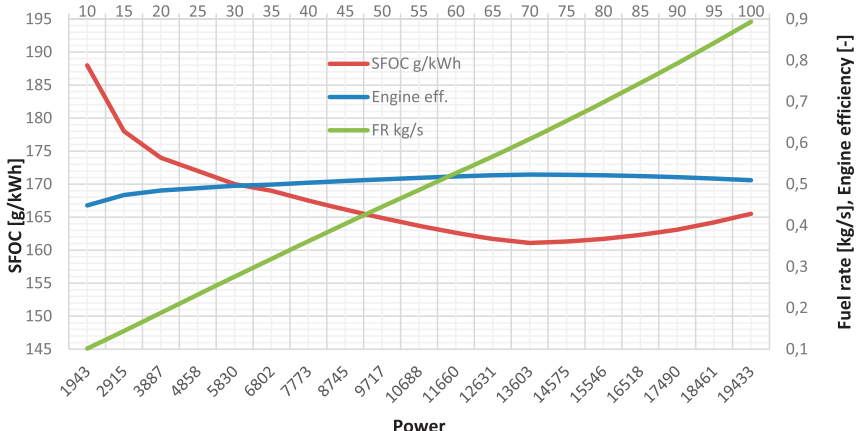

Fig. 6. Specific fuel consumption, fuel rate and engine efficiency

The geometry of the engine and its components is available from the Computerized Engine Application System (CEAS), as well as the Project Guide of the selected engine [74, 75]. Two selected drawings are shown in Fig. 7. Based on these drawings, all necessary geometric parameters of the engine can be specified. These parameters are given in Table 3.

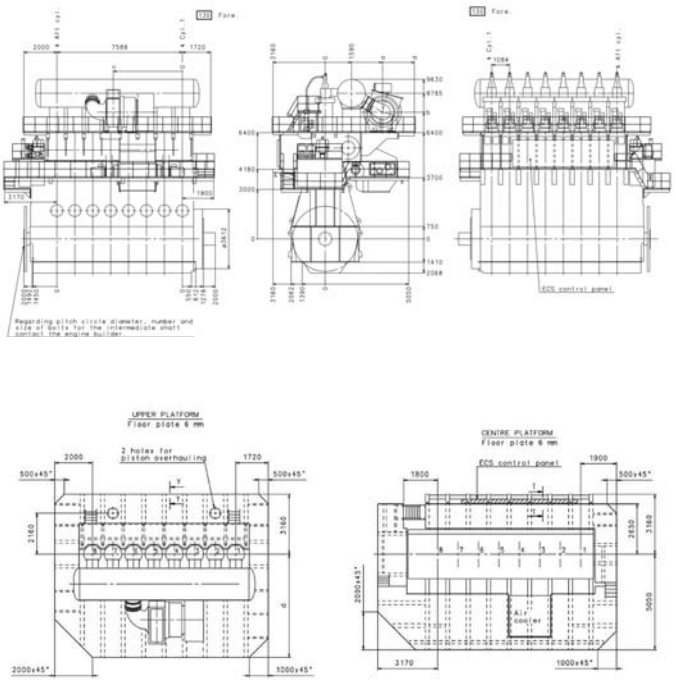

Fig. 7. Outline drawings of MAN B&W 8S65ME-C8.5-TII Engine, [74, 75]

Table 3. The necessary parameters of MAN-B&W 8S65ME-C8.5-TII engine for modelling, [74, 75]

Parameter	Unit	Value
Volume of the inlet air manifold	[m³]	26.000
Volume of the exhaust gas receiver	[m³]	20.313
Diameter of the cylinders	[m]	0.650
Stroke	[m]	2.730
Charge air cooler efficiency	[%]	88.68
Temperature of the inlet cooling water	[°C]	25

The rate of operation, pressure ratio, efficiency, dimensions, weights, and other parameters of the MAN B&W High Eff. TCA88 turbocharger can be found in its publicly available manual and Project Guide [76]. Based on these data the average radius of the compressor wheel is 0.354 m. The compressor map with the related values is not available in the mentioned references and therefore a similar compressor, of which the map was presented in Fig. 3, is selected and then scaled for the applied turbocharger. Referring to Eqs. (19) to (22), the look-up table for the parameters $\dot{v}_{C1}$, β_{C1} and β_{C2} is given in Table 4

Table 2. MAN-B&W 8S65ME-C8.5 engine performance at steady states at different operating points (OP) of SMCR, [74, 75]

Load	Power	Speed	SFOC	FR	Engine eff.	Ex. gas temp.	Ex. gas amount
OP [%]	[kW]	[rpm]	[g/kWh]	[kg/s]	[-]	[°C]	[kg/s]
10	1943	43.1	188.0	0.101468	0.4485	165	9.9
15	2915	49.3	178.0	0.144131	0.4736	203	11.6
20	3887	54.3	174.0	0.187872	0.4845	219	13.9
25	4858	58.5	172.0	0.232104	0.4902	223	16.3
30	5830	62.1	170.0	0.275306	0.4959	217	19.3
35	6802	65.4	169.0	0.319316	0.4989	259	18.7
40	7773	68.4	167.5	0.36166	0.5033	251	21.2
45	8745	71.1	166.1	0.403485	0.5076	242	23.7
50	9717	73.7	164.9	0.445093	0.5113	234	26
55	10688	76.0	163.7	0.486007	0.5150	228	28.2
60	11660	78.3	162.6	0.526643	0.5185	224	30.4
65	12631	80.4	161.7	0.567342	0.5214	221	32.4
70	13603	82.4	161.1	0.608734	0.5233	220	34.4
75	14575	84.3	161.3	0.653041	0.5227	220	36.2
80	15546	86.1	161.7	0.698275	0.5214	221	38
85	16518	87.9	162.3	0.744687	0.5195	224	39.6
90	17490	89.6	163.1	0.792394	0.5169	228	41.2
95	18461	91.2	164.2	0.842027	0.5135	234	42.8
100	19433	92.8	165.5	0.893378	0.5094	241	44.3

Table 4. Parameters for identifying the selected compressor map

Compressor tip speed [m/s]	$\dot{v}_{C1}$	β_{C1}	β_{C2}
50	-5	25	1
100	-1.685006140	22.09147846	1.089617728
150	1.107917327	19.85276203	1.168744389
200	2.876162550	22.66164200	1.336188092
250	4.716031731	15.85172281	1.558461663
300	5.897304273	16.081286 0	1.870132421
350	9.25198641	9.443337977	2.267474338
400	11.78456552	6.429917587	2.809177986
425	13.16459085	4.743205422	3.156624514
450	13.89641087	5.975417504	3.518829733

To set the pressure of the intake air manifold/receiver for the first iteration, p_{am}, (Section "Setting Up the Model Parameters", part C, Point 7) the following empirically obtained second-order polynomial is used:

$$p_{am}(OP) = \left(-0.00001 \cdot OP^2 + 0.0024 \cdot OP + 1\right) \cdot p_{gr} \quad \textbf{(99)}$$

To calculate the air pressure after the compressor, Eq. (24), it is necessary to adjust the pressure increase due to the application of auxiliary blowers (if installed), Δp_{blr}, pressure dropping in the charge air cooler, p_{clr}, and the dynamic pressure at the compressor outlet, p_{dyn}. Having in mind Eq. (26) and (36), the following constants are applied, which are calculated empirically by selecting a series of the low-speed long-stroke supercharged diesel engines produced by MAN-B&W: $a_{dyn} = 0.01$, $a_{clr} = 0.15425$ and $a_{clr} = 0$ (no blower is included in the system). The efficiency of the charge air cooler is calculated for different operating points at steady states and the average value is applied. This average value is 88.68%.

Next, by taking into account the selected compressor map, the compressor tip speed is determined as a second-order function of the operating point as follows (see Section "Setting Up the Model Parameters", part C, Point 7):

$$u_{TC}(OP) = \left(0.027372 \cdot OP^2 + 6.942 \cdot OP + 20.334\right) \cdot p_{gr} \quad \textbf{(100)}$$

The filling efficiency is a function of the operating point. When no data is available, it can be considered as 0.9. However, it should be identified after adjusting k_b (see Eq. (60)) to assure that the determined temperature of the exhaust gases after the cylinders, T_4, satisfies its initiated value in respect to the steady-state data.

The data needed for calculating the NOx emissions are based on the values given in Table 5.

Table 5. Molar concentrations of elements and compounds in the atmospheric air

Gas		Average percentage share in the atmosphere [%]	Concentration [mol/cm^3]	Molar mass [g/mol]
Nitrogen	N_2	78.084	$3.48 \cdot 10^{-5}$	28.02
Oxygen	O_2	20.946	$9.35 \cdot 10^{-6}$	32
Argon	Ar	0.9340	$4.17 \cdot 10^{-7}$	40
Carbon dioxide	CO_2	0.0360	$1.6 \cdot 10^{-8}$	44
Nitric oxide	NO	0.0003	$1.34 \cdot 10^{-10}$	30
Hydrogen	H_2	0.0005	$2.23 \cdot 10^{-10}$	2

SIMULATION AND VALIDATION

The simulations are conducted for the range of 10% to 100% of SMCR, where the fuel flow rate firstly changed from the respected value for 100% of SMCR to a lower selected level decreased by 10% each time. Next, the fuel flow rate again increased from the given lower level to 100% of SMCR. The validation is checked regarding the consistency of the initial and final values, as well as the consistency of the values of variables at each operating point with the steady state data delivered by the engine manufacturer. Each of three simulation phases lasts 50 seconds. It should be noted that the simulation results presented here are for those parameters that were adjusted after the first iteration of the set-up process explained under "Setting Up the Model parameters".

The selected variables are:

1. Fuel flow rate (input in respect to the operating point)
2. Flow rate of air after compressor
3. Flow rate of air into cylinders
4. Flow rate of air that takes part in combustion
5. Flow rate of exhaust gases after cylinders
6. Flow rate of exhaust gases into turbine
7. Temperature of air after compressor
8. Temperature of air into cylinders
9. Temperature of air that takes part in combustion
10. Temperature of exhaust gases into turbine
11. Temperature of exhaust gases after turbine
12. Pressure ratio of compressor
13. Pressure ratio of turbine
14. Tip speed of compressor wheel
15. Power of compressor
16. Power of turbine
17. Angular velocity of turbocharger shaft
18. Mass of air in intake air manifold
19. Temperature of air in intake air manifold
20. Pressure of air in intake air manifold
21. Mass of gases in exhaust gas receiver
22. Temperature of gases in exhaust gas receiver
23. Pressure of gases in exhaust gas receiver
24. Torque of propeller
25. Torque of engine
26. Power of engine
27. Angular velocity of engine shaft
28. Fuel-to-air ratio
29. Formation rate of nitric oxide

These variables have been illustrated in Figs. 8 to 14. The first figure shows the changing of the fuel flow rate as input and the other figures are the system responses. For the sake of clarity, the responses are presented only in the time interval between 40 seconds and 140 seconds. Similarly, for the turbocharger only 4 operating points were presented to keep the clarity of the figures. Moreover, as the rate of formation of nitric oxide rapidly changes in time, the figures are presented for shorter periods, when the fuel rate is changed at 50 seconds and 100 seconds.

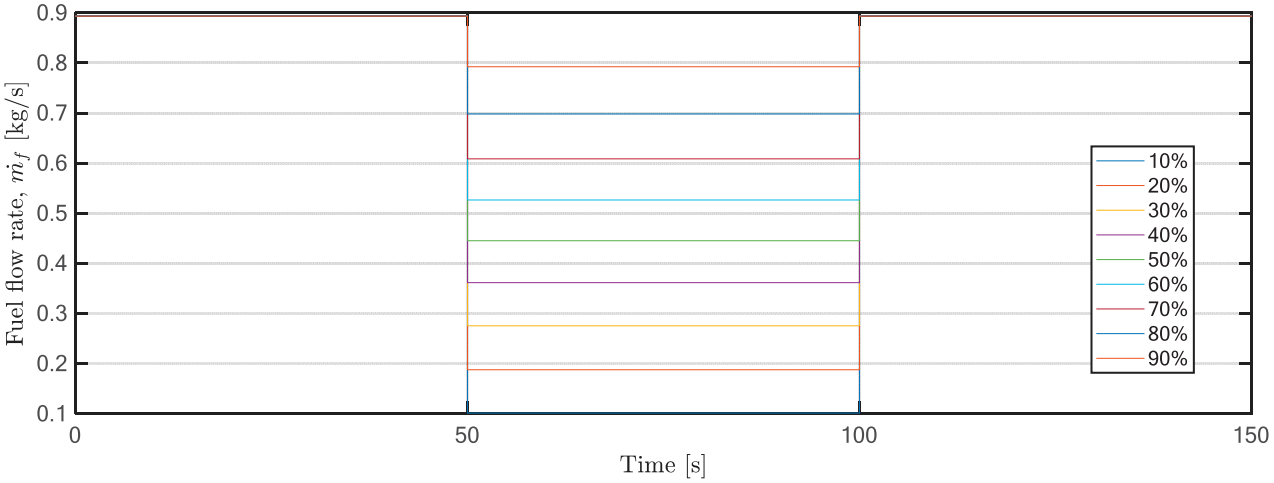

Fig. 8. Fuel flow rate as input

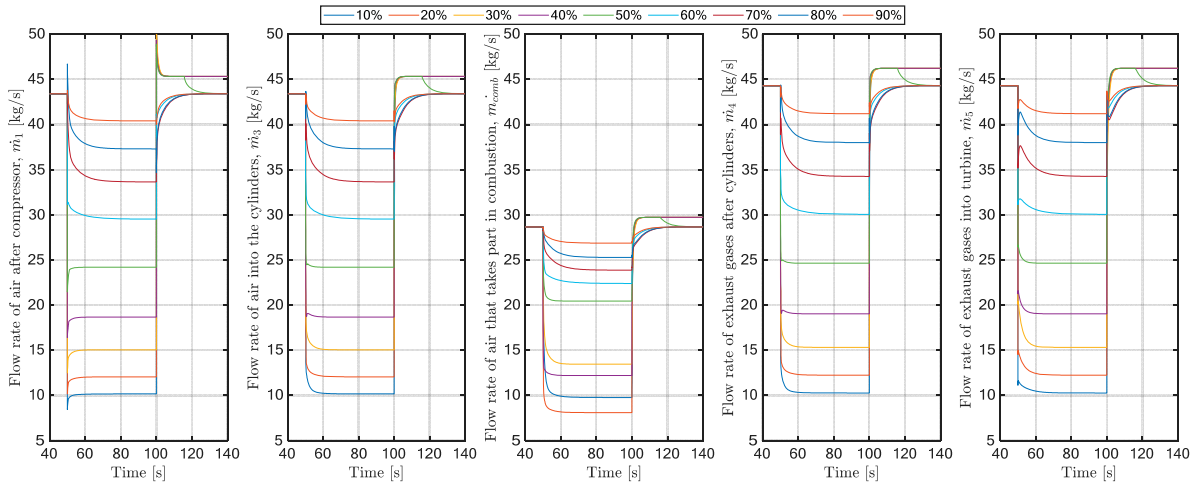

Fig. 9. Mass flow rates

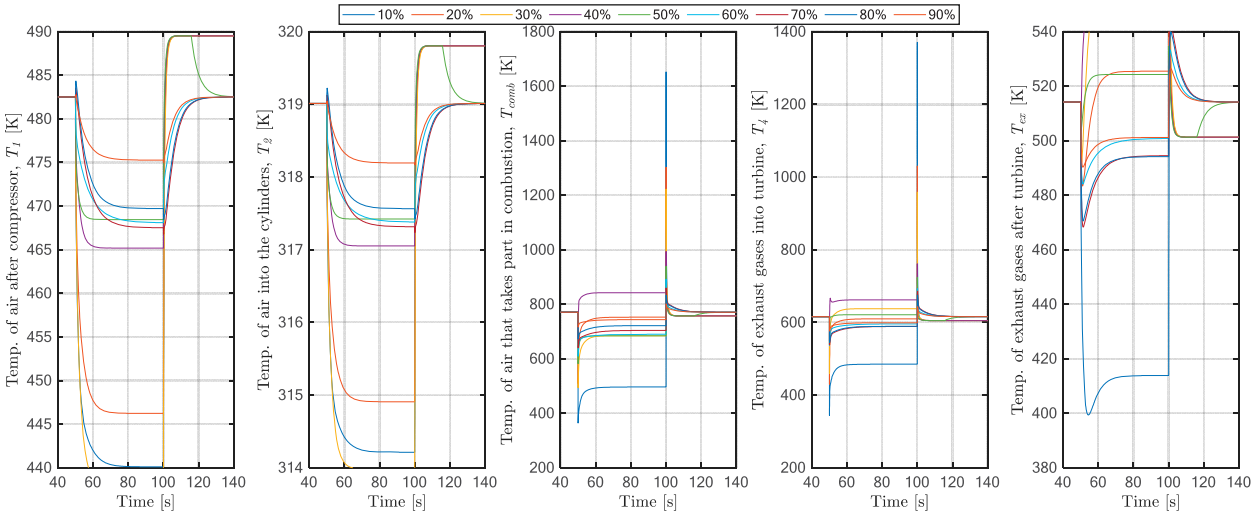

Fig. 10. Temperatures

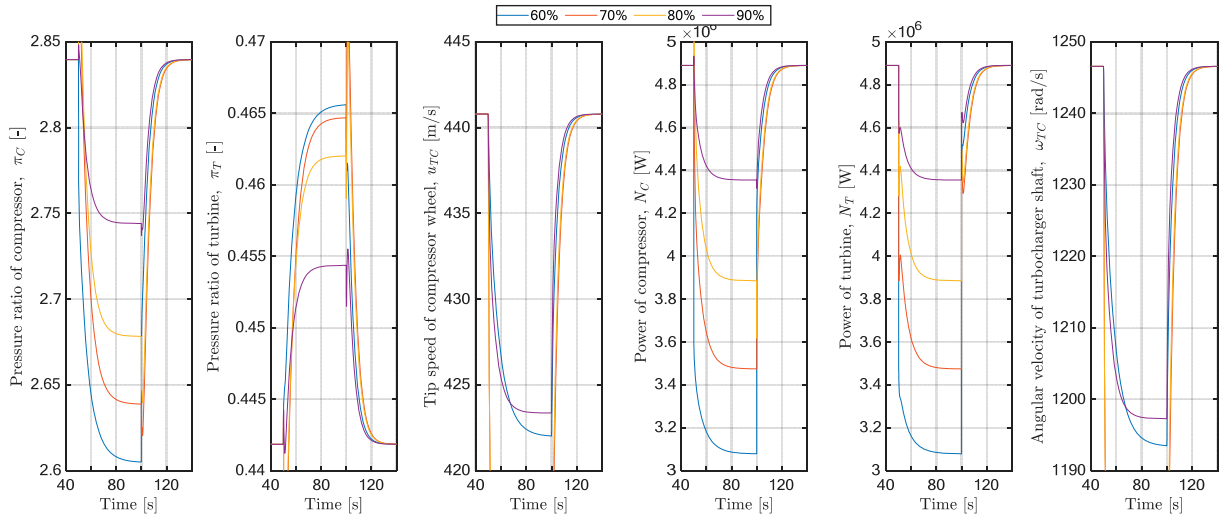

Fig. 11. Turbocharger variables for changing of fuel rate in respect of four operating points

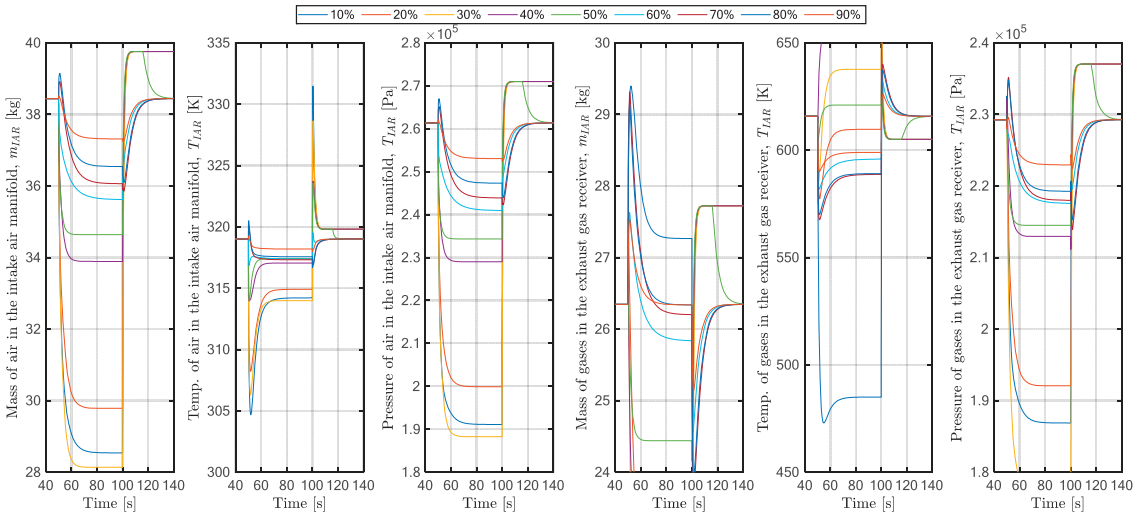

Fig. 12. Variables of inlet air manifold and exhaust gas receiver

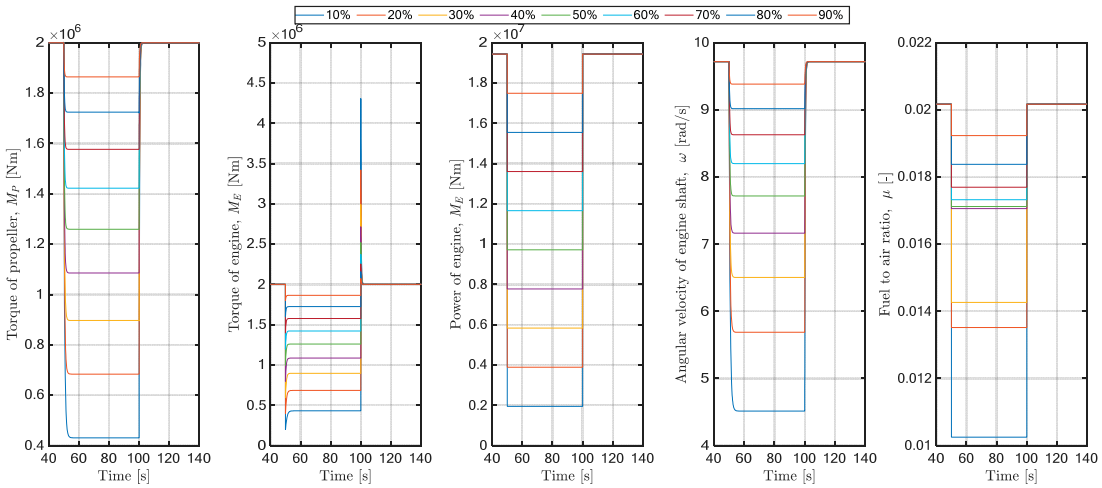

Fig. 13. General variables of engine and propeller

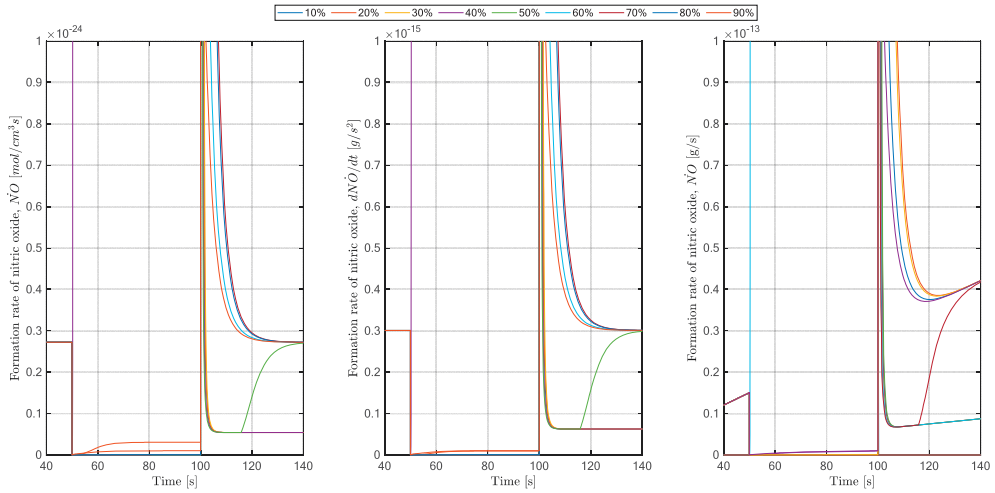

Fig. 14. Rate of formation and accumulated sum of emitted nitric oxide

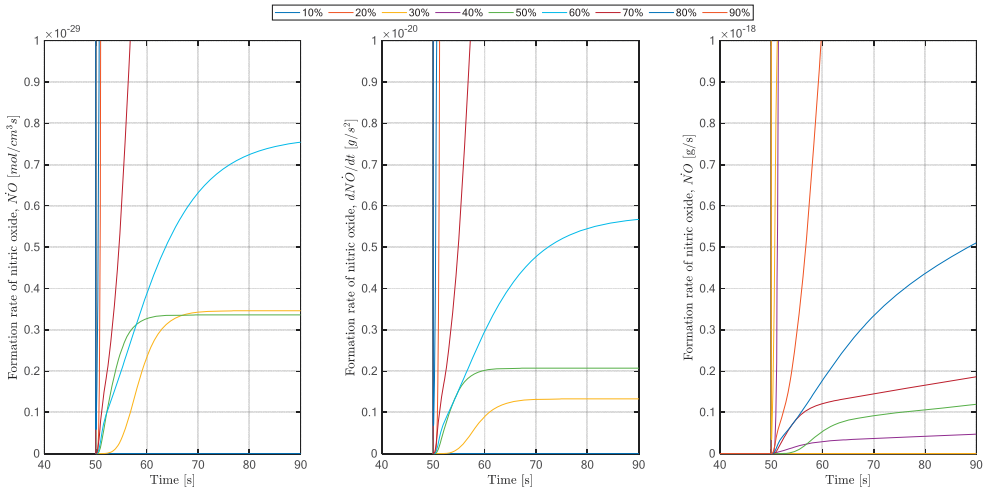

Fig. 14 (continued). Rate of formation and accumulated sum of emitted nitric oxide

To validate the result, the least accurate results, i.e. those are obtained after the 1st trial, are selected and presented, which are obtained using the adjusted system parameters after the first iteration. Based on these results, 7 variables among the 29 did not satisfy the first and the second conditions of consistency mentioned before, i.e., they do not return to the related values to 100% of SMCR at the end of simulation or their values at steady state are not equal to the respected values delivered in the engine project guide provided by the manufacturer. They are: temperature of exhaust gases after the turbine, and mass, temperature and pressure of the air in the inlet air manifold or the exhaust gases in the exhaust gases receiver. Of course, only a few variables are available from the project guides, which can be compared to the simulation results. Three of them are shown in Fig. 15. The conditions are not satisfied only for a narrow range of operating points, between 40% and 60% of SMCR, except the temperature of exhaust gases after turbine (see Fig. 15). The values of the latter are consistent only for operating points above 50 (50% of SMCR). On the other hand, the relative error in all cases, except the temperature of exhaust gases after turbine, is not more than 4%. Therefore, it can be concluded that the applied method, even at the first iteration, gives acceptable results and the presented model and adjusted parameters are generally verified. Better results are achieved after 3rd trial but they are not presented here.

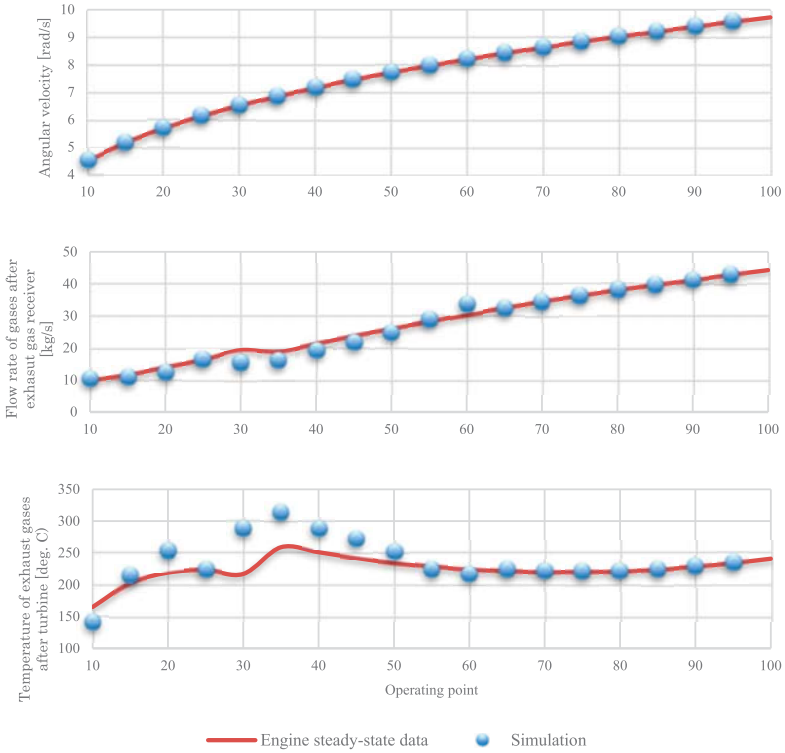

Fig. 15. Comparison of the engine steady-state data given by the manufacturer in the project guide with the simulation results

CONCLUSION

The development of a ship motion model as an overall system, with interacting subsystems such as the hull, propeller, engine and rudder, demands the use of a suitable mathematical model of the engine that is able to provide enough information not only about the torque and power but for internal events of marine diesel engines. These internal variables may have significant influences on the performance of ship propulsion systems. Different phenomena such as vibrations, emissions, structural failures and fatigue, ship control, etc. are also directly related to these variables. This requires an appropriate mathematical model of the engine. The mean-value quasi-steady zero-dimensional model seems to be the most suitable option for the mentioned investigations. However, given the lack of information to set up the parameters needed for the selected engine, it is impossible to easily imbed this type of model into the above-mentioned overall model. This paper is an answer to this need and presents how the model should be built, and its parameters can be determined using only publicly available data and without any experimental stand tests. The paper includes the fundamentals of the model, the algorithm of preparing the simulation model, and the procedure of determining the model parameters. A case study is selected and simulations are conducted. For 29 selected variables of the system the results of the simulation have been presented and then verified mainly against steady-state data. The method used for determining the system parameters is based on trial and error. However, it is shown that by using the presented method, even after the first iteration, the relative error is low. This conclusion legitimizes the use of the model and the method for further analyses, wherever rapid modelling of a marine diesel engine is needed.

REFERENCES

1. Wang F., Pulsation Signals Analysis of Turbocharger Turbine Blades Based on Optimal EEMD And TEO, Polish Maritime Research 3 (103) 2019 Vol. 26; pp. 78-86 10.2478/pomr-2019-0048.

2. Ghaemi M. H., Zeraatgar H., Analysis of Hull, Propeller and Engine Interactions in Regular Waves by a Combination of Experiment and Simulation, Journal of Marine Science and Technology, 26, pages 257–272, 2021.

3. Gu X., Jiang G., Guo Z., Ding S., Design and Experiment of Low-Pressure Gas Supply System for Dual Fuel Engine, Polish Maritime Research 2 (106) 2020 Vol. 27; pp. 76-84 10.2478/pomr-2020-0029.

4. Cepowski T., Regression Formulas for The Estimation of Engine Total Power for Tankers, Container Ships and Bulk Carriers on the Basis of Cargo Capacity and Design Speed, Polish Maritime Research, 1 (101) 2019 Vol. 26; pp. 82-94 10.2478/pomr-2019-0010

5. Yang Z., Tan Q., Geng P., Combustion and Emissions Investigation on Low-Speed Two-Stroke Marine Diesel Engine with Low Sulfur Diesel Fuel, Polish Maritime Research, 1 (101) 2019 Vol. 26; pp. 153-161 10.2478/pomr-2019-0017

6. Zeraatgar H., Ghaemi M. H., The Analysis of Overall Ship Fuel Consumption in Acceleration Manoeuvre using Hull-Propeller-Engine Interaction Principles and Governor Features, Polish Maritime Research 1 (101) 2019 Vol. 26; pp. 162-173 10.2478/pomr-2019-0018

7. Gajek J., Marine Propulsion System Simulator of a CPP (Symulator Okrętowego Układu Napędowego ze Śrubą Nastawną – in Polish), Budownictwo Okrętowe, March 1975.

8. Andersen T.E., On Dynamics of Large Ship Diesel Engine, PhD Thesis, Technical University of Denmark, 1974.

9. Roszczyk S., et al, Static and Dynamic Characteristics of Marine Generating Sets (Statyczne i Dynamiczne Własności Okrętowych Zespołów Prądotwórczych – in Polish), Wydawnictwo Morskie, Gdansk, 1976.

10. Tittenbrun S., Kowalski Z., Łastowski W. F., Characteristics of Rotational Speed Regulators of Ship Diesel Engines under the Light of Testing on Simulation Stands (Własności Regulatorów Prędkości Obrotowej Okrętowych Wysokoprężnych Silników Spalinowych w Świetle Badań na Stanowiskach Symulacyjnych – in Polish), Budownictwo Okrętowe, Dec. 1979.

11. Kowalski Z., Simulation Study of Ship Propulsion Subsystems (Badanie Symulacyjne Podsystemów Napędowych Statków – in Polish), Zeszyt Naukowe Politechniki Gdańskiej (Elektryka), No. 49, Poland, 1980.

12. Krutov V. I., Automatic Control of Internal Combustion Engines, Mir Publishers, Russia, 1987.

13. Blanke M., Andersen J. S., On Dynamics of Large Two Stroke Diesel Engines: New Results from Identification, Proceedings of 9th IFAC World Conference, Budapest, Hungry, 1984.

14. Lam W. C., Katagi T., Hashimoto T., Simulation of Transient Behaviour of Marine Medium Speed Diesel Engine, 3rd International Conf. of MCMC, Southampton, Sept. 1994.

15. Ferenc M., Numerical modeling of the Control Process of the Marine Diesel Engine with Consideration of Non-linearity (Modelowanie Numeryczne Procesu Regulacji Okrętowego Silnika Wysokoprężnego z uwzględnieniem nieliniowości – in Polish), Zeszyty Naukowe Politechniki Śląskiej, No. 567, 1978.

16. Ferenc M., Osuch W., Stokloska H., A simplified Mathematical Model of the Dynamics of a Medium Speed Diesel Engine (Uproszczony Model Matematyczny Dynamiki Średnioobrotowego Silnika Wysokoprężnego – in Polish), Silniki Splalinowe 4/89, Poland, 1989.

17. Ferenc M., Wideł S., Fiutkowski M., Principles for Selecting the Dynamic Characteristics of the Rotary Speed Controller for a Medium-Speed Diesel Engine Driving a Generator (Zasady Doboru Charakterystyki Dynamicznej Regulatora Prędkości Obrotowej Średnioobrotowego Silnika Wysokoprężnego Napędzającego Prądnicę, Silniki Spalinowe – in Polish), No. 3 '90. 1990.

18. Smith J. R., et al., Prediction of Dynamic Response of Marine System Incorporating Induction-Motor Propulsion Drives, Proc. IEE, Vol. 127, No. 5, Sept. 1980.

19. Taylor S. K., et al., The Predetermination of the Dynamic Response of Marine Systems Powered by Parallel Connected Gas Turbine and Diesel Generators, CIMAC 1985, paper D56, Oslo, 1985.

20. Ford M. P., A Simplified Turbocharged Diesel Engine Model, Proceedings IMechE, Vol. 201, paper D4, 1987.

21. Woodward J. B., Lattore R. G., Simulation of Diesel Engine Transient Behaviour in Marine Propulsion Analysis, Report MA-RD-940-83032, US Department of Transportation, Maritime Administration, 1983.

22. Woodward J. B., Lattore R. G., Modelling of Diesel Engine Transient Behaviour in Marine Propulsion Analysis, SNAME Transactions, Vol. 192, 1984.

23. Hendricks E., Chevalier A., Emerging Engine Control Technologies, Technical University of Denmark, 1985.

24. Hendricks E., Poulsen N. K., Minimum Energy Control of a Large Diesel Engine, SAE Technical Paper Series 861191, 1986.

25. Hendricks E., The Analysis of Mean Value Engine Models, SAE Technical Paper Series 890563, 1989.

26. Hendricks E., Mean Value Modelling of Large Turbocharged Two-Stroke Diesel Engines, SAE Technical Paper Series 890564, 1989.

27. Jansen J. P., et al., Mean Value Modelling of a Small Turbocharged Diesel Engine, SAE Tech-nical Paper Series 910070, 1991.

28. Woud J. K., Boot P., Riet B. J., A Diesel Engine Model for the Dynamic Simulation of Propulsion Systems, Schip en Werf de Zee, Vol. 3, pp. 4-13, Jan. 1993.

29. Próchnicki W., Model Matematyczny Układu Turbozespół Dowadowający - Silnik Spalinowe Przeznaczone do Badań Zmiennych Warunków Ruchu Zespołu Napędowego Statku, Praca Badawcza Nr. 86/93, Wydz. O. i O., Politechnika Gdanska, Gdansk, 1993.

30. Próchnicki W., Modified System of Cooperation Between Turbocharger and Diesel Engine in Transient States, 1st International Symposium on Automatic Control of Ship Propulsion and Ocean Engineering Systems, Gdansk, 1994.

31. Próchnicki W., Dzida M., Badania Wstępne Układu Turbozespół Doładowujący Silnik Spali-nowy w Zmiennych Warunkach Ruchu Zespołu Napędowego Statku, Praca badawcza No. 58/94, W. O. i O., Politechnika Gdańska, Poland, 1993.

32. Kafar J., Mathematical Model of Dynamic Behaviour of a Diesel Engine in Propulsion System, Polish Maritime Research, No. 2/94, Poland, 1994.

33. Lan W. C., Katagi T., Hashimoto T., Quasi Steady State Simulation of Diesel Engine Transient Performance and Design of Mechatronic Governor, Bulletin of MarEng Society of Japan, Vol. 24, No. 1, Feb. 1996.

34. Olsen D. R., Simulation of a Free-Piston Engine with Digital Computer, SAE Trans., Vol. 66, pp. 668-682, 1958.

35. Cook H. A., Analysis and Interpretation of Turbo-charged Diesel Engine Performance, SAE Trans., Vol. 67, 1959.

36. Whitehouse N. D., et al., Methods of Predicting Some Aspects of Performance of a Diesel Engine Using a Digital Computer, Proc. IMechE, Vol. 176, No. 9, 1962.

37. Borman G. L., Mathematical Simulation of Internal Combustion Engine Processes, PhD Thesis, University of Wisconsin, 1964.

38. Streit E.E., Mathematical Simulation of Large Pulse-Turbocharged Two-Stroke Diesel Engine, PhD Thesis, University of Wisconsin, 1970.

39. Streit E.E., Mathematical Simulation of Large Pulse-Turbocharged Two-Stroke Diesel Engine, PhD Thesis, University of Wisconsin, 1970.

40. Marzouk M., Some Problems in Diesel Engine Research with Reference to Computer Control and Data Acquisition, Proc. IMechE, Vol. 190, No. 23/76, 1976.

41. Benson S., The Thermodynamics and Gas Dynamics of Internal Combustion Engine, Vol. I, Oxford, Clarendon Press, 1982.

42. Woschni G., Anisits F., Experimental Investigation and Mathematical Presentation of Rate of Heat Release in Diesel Engine Dependent upon Engine Operating Conditions, SAE Technical Paper Series 740086, 1974.

43. Woschni G., A Universally Applicable Equation for the Instantaneous Heat Transfer Coefficient in the Internal Combustion Engine, SAE Technical Paper Series 670931, 1967

44. Wiebe I., Halbempirische Formel für die Verbrennungsgeschwindigkeit, Velage de Akademic der Wissenschaften der VdSSR, Moscow, 1967.

45. Watson N., Marzouk M., A Non-Linear Digital Simulation of Turbocharged Diesel Engines under Transient Conditions, SAE Technical Paper Series 770123, 1977.

46. Watson N., Janota M. S., Turbocharging the Internal Combustion Engine, MacMillan Publish-ers Ltd., London, 1982.

47. Banisoleiman K., Bazari Z., Smith L. A., Mathieson N., Simulation of Diesel Engine Per-formance, Trans. IMarE, Vol. 105, pp. 117-135, 1993.

48. Larmi M. J., Transient Response Model of Low Speed Diesel Engine in Ice-Breaking Cargo Vessels, PhD Thesis, Helsinki University of Technology, Helsinki, 1993.

49. Ghaemi M. H.: Changing the Ship Propulsion System Performances Induced by Variation in Reaction Degree of Turbocharger Turbine, Journal of Polish CIMAC, Vol. 6., No.1 (2011), pages 55-70.

50. Benson R. S., Wave Action in the Exhaust System of a Supercharged Two-Stroke Engine Model, International Journal of Mechanical Science, Vol. 1, p. 253, 1959.

51. Benson R. S., et al., A Numerical Solution of Unsteady Flow Problems, International Journal of Mechanical Science, Vol. 6, pp. 117-144, 1964.

52. Benson R. S., Woods W. A., Woollat D., Unsteady Flow in Simple Branch Systems, Proc. IMechE, Vol. 178, Pt. 3I(iii), 1963/4.

53. Blair G. P., Arbuckle J. A., Unsteady Flow in the Induction System of a Reciprocating Internal Combustion Engine, SAE 700443, 1970.

54. Blair G. P., Goulburn J. R., The Pressure Time History in the Exhaust System of a High Speed Reciprocating Internal Combustion Engine, SAE 67077, 1967.

55. Blair G. P., McConnel H. J., Unsteady Gas Flow Through High Specific Output Four-Stroke Cycle Engines, SAE 740736, 1974.

56. Bazari Z., A DI Diesel Combustion and Emission Predictive Capability for Use in Cycle Simulation, SAE Technical Paper Series 920462, 1992.

57. Sujesh G., Ramesh S., Modeling and control of diesel engines: A systematic review, Alexandria Engineering Journal, Vol. 57, Issue 4, pp. 4033-4048, 2018, ISSN 1110-0168, https://doi.org/10.1016/j.aej.2018.02.011 (https://www.sciencedirect.com/science/article/pii/S1110016818301984)

58. Lee B., Jung D., Kim Y. W., Physics-Based Control Oriented Mean Value Model for Diesel Combustion Process with EGR Sensitivity, Proceedings of the ASME Dynamic Systems and Control Conference, 2011, pp. 1-8.

59. Hendricks E., and Sorenson S., Mean Value SI Engine Model for Control Studies, American Control Conference, 1990, pp. 1882-1887.

60. Sengupta S., De S., Bhattacharyya A. K., Mukhopadhyay S., Deb A. K., Fault Detection of Air Intake Systems of SI Gasoline Engines using Mean Value and Within Cycle Models, 5th Annual IEEE Conference on Automation Science and Engineering, Bangalore, 2009, pp. 361-366.

61. Yacoub Y., Mean Value Modeling and Control of a Diesel Engine Using Neural Networks, Dr. of Mechanical Engineering Dissertation, West Virginia University, Morgantown, USA, 1999.

62. Theotokatos G. P., A Modeling Approach for the Overall Ship Propulsion Plant Simulation, 6th WSEAS International Conference on System Science and Simulation in Engineering, Venice, 2007, pp. 80-87.

63. Guzzella L., Onder C.H., Introduction to Modeling and Control of Internal Combustion Engine Systems, Springer, 2010.

64. Yum K. K., Modeling and Simulation of Transient Performance and Emission of Diesel Engine, NTNU - Trondheim 2012, pp. 64-68.

65. Scappin F., Stefansson S. H., Haglind F., Andreasen A., Larsen U., Validation of a zero-dimensional model for prediction of NOx and engine performance for electronically controlled marine two-stroke diesel engines, Applied Thermal Engineering, Volume 37, May 2012, Pages 344-352 2012.

66. Kharroubi K., Chen H., A Semi-Experimental Modeling Approach for a Large Two-Stroke Marine Diesel Engine Simulation, 27th CIMAC World Congress, Shanghai, China, May 13-16, 2013, Paper no. 105.

67. Baldi F., Theotokatos, G., Andersson K., Development of a combined mean value-zero dimensional model

and application for a large marine four-stroke diesel engine simulation, https://www.researchgate.net/publication/277338414_Development_of_a_combined_mean_value-zero_dimensional_model_and_application_for_a_large_marine_four-stroke_Diesel_engine_simulation

68. Altosole M., Campora U., Figari M., Laviola M., A Diesel Engine Modelling Approach for Ship Propulsion Real-Time Simulators, 2019, https://www.mdpi.com/2077-1312/7/5/138/pdf

69. Zimmer K., Aufladung von Verbrennungsmotoren, 1985, ISBN: 978-3-540-15902-5, https://citations.springernature.com/book?doi=10.1007/978-3-662-05913-5

70. Streuli A., Application of the BBC Power Turbine, BBC Brown Boveri, 1985.

71. Polish Norm PN-M-01521:1993, "Silniki spalinowe tłokowe – Terminologia".

72. Chen S. K., Flynn P., Development of a Compression Ignition Research Engine, SAE 650733, 1965.

73. Heywood J. B., Internal Combustion Engine Fundamentals, McGraw-Hill, 1988.

74. MAN-B&W Computerized Engine Application System (CEAS), https://www.man-es.com/marine/products/planning-tools-and-downloads/ceas-engine-calculations.

75. MAN B&W S65ME-C8.5-TII Project Guide Electronically Controlled Two-stroke Engines, online: https://www.academia.edu/35674638/MAN_B_and_W_S90ME_C8_TII_Project_Guide_Electronically_Controlled_Two_stroke_Engines

76. TCA Turbocharger, The Benchmark, online: https://turbocharger.man-es.com/docs/default-source/shopwaredocuments/tca-turbochargerf451d068cde04720bdc9b8e95b7c0f8e.pdf?sfvrsn=81b197c6_3, & Project Guide TCA Turbocharger, online: https://turbocharger.man-es.com/docs/default-source/shopwaredocuments/tca.pdf?sfvrsn=98c91c09_2.

APPENDIX A

AIR AND EXHAUST GAS PROPERTY RELATIONSHIPS

Tabulated data or algebraic expressions are required for the partial derivative of the internal energy u, with respect to the temperature and air-to-fuel ratio (and pressure, if dissociation is not to be neglected) and gas constant, R. Relationships are required for air, combustion products and the mixture of the two. By derivative general algebraic expressions for combustion products in terms of the fuel-to-air ratio, the properties of mixtures of air or combustion products may be evaluated by using the appropriate overall value of the fuel-to-air ratio or equivalence ratio (F=0 for pure air).
A homogeneous mixture and equilibrium thermodynamic properties for the products of combustion are assumed. Rather than go through the full thermodynamics of combustion product calculations at each step, it is common to use algebraic expressions curve-fitted to the result of such calculations. Several algebraic expressions are available, of which one is as follows [Benson 1982]:

$$u = K_1(T) - K_2(T) \quad [\text{kJ/kgK}] \tag{A.1}$$

where

$$K_1(T) = 0.692T + 39.17\times10^{-6}T^2 + 52.9\times10^{-9}T^3 + \\ - 228.62\times10^{-13}T^4 + 277.58\times10^{-17}T^5 \tag{A.2}$$

$$K_2(T) = 3049.39 - 5.7\times10^{-2}T - 9.5\times10^{-5}T^2 + \\ + 21.53\times10^{-9}T^3 + 200.26\times10^{-14}T^4 \tag{A.3}$$

and the gas constant is given by

$$R = 0.287 + 0.02F \quad [\text{kJ/kgK}] \tag{A.4}$$

(per kg of original air).

The stoichiometric fuel-to-air ratio is 0.0676, hence the above expressions must be divided by (1+0.0676F) if the value of u or R is required per unit mass of combustion products.
In Figs. A.1, A.2 and A.3, the specific heat at constant pressure, specific internal energy and specific enthalpy are plotted, respectively. Specific enthalpy was derived by integration of the specific heat. Specific enthalpy was set as zero at 298.15 K.

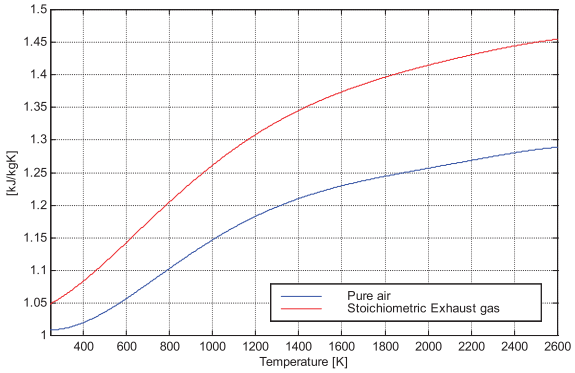

Fig. A.1. Heat capacity at constant pressure

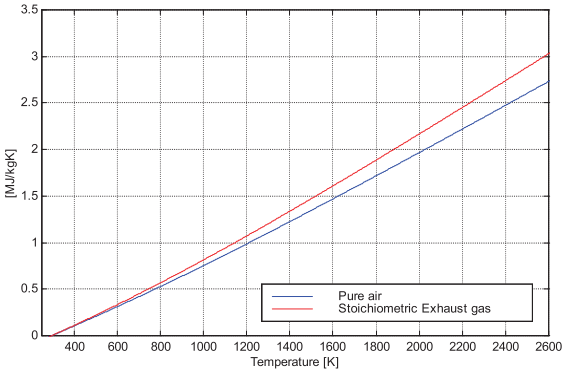

Fig. A.2. Specific enthalpy

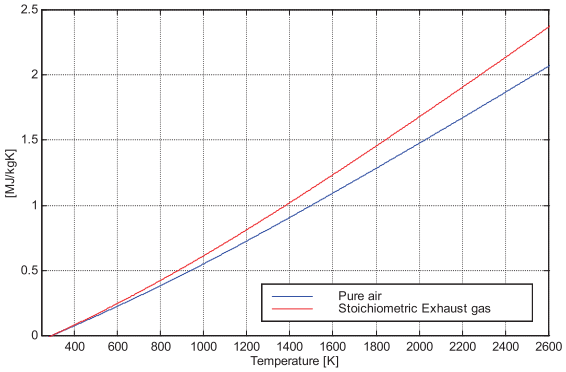

Fig. B.3. Specific internal energy

CONTACT WITH THE AUTHOR

Mohammad Hossein Ghaemi
e-mail: ghaemi@pg.edu.pl

Gdańsk University of Technology
Narutowicza 11/12
80-233 Gdańsk
Poland